Chapter 4

VOLTAGE STABILITY ENHANCEMENT AND LOSS REDUCTION UNDER PRESENCE OF P/Q AND PQV BUSES

4.1 INTRODUCTION

Conventional power system usually consists of PQ and PV buses apart from slack bus. In recent years, the researchers have worked on the systems with presence of novel sets of buses known as P, Q and PQV buses. A P bus is defined as a generation bus that has specified real power generation but unknown reactive power generation, voltage magnitude and voltage angle. A Q bus is defined as a generation bus that has specified reactive power generation, but unknown real power generation, voltage magnitude and voltage angle. The real power injection is fixed at the P bus while reactive power injection is fixed at the Q bus. A PQV bus is defined as a bus with specified real power generation, reactive power generation and voltage magnitude but unknown voltage angle. The only unknown variable at the PQV bus is voltage angle. The voltage magnitude at the PQV bus may be regulated through control of reactive power injection at P buses and control of real power injection at the Q buses [165]–[167]. This is achieved through connection of variable reactive power source at P buses and variable real power source at Q buses. The pre-defined voltage magnitude at PQV bus may be obtained by varying reactive power injection at P bus and/or real power injection at Q bus. In recent works loss minimization and network reconfiguration have been performed through control of voltage at remotely located PQV bus to a fixed value by varying reactive power injection at the selected P bus [64], [168].

Literature review reveals that loadability enhancement of distribution system so far studied by various authors has been done with the PQ and PV buses present in the system, no work has been found to study loadability enhancement considering P/Q, PQV buses in the system. Control of voltage at remotely located PQV bus through regulation of reactive power/ real power injection at P/Q bus may play an effective role in voltage stability enhancement and network loss reduction. Hence, in this work, effect of P/Q and PQV buses in enhancing system voltage stability in terms of maximum loadability as well as loss reduction have been studied. Impact of network reconfiguration and DG placement in voltage stability enhancement and loss minimization was presented in last chapter. Objective of the work carried out in this chapter is to further enhance voltage stability margin and minimize power loss in the network through network reconfiguration and different types of DGs allocation in presence of P/Q and PQV buses. Grey Wolf Optimizer (GWO) tool has been utilized to achieve the optimal solution for the objective function formulated.

4.2 REFORMULATION OF NRLF EQUATION UNDER PQV AND P/Q BUSES

4.2.1 NRLF Equation under PQV and P buses

Existence of pair of PQV and P buses in network may be solved by redefining the Jacobian matrix. A P bus is introduced as a reactive power source with unknown reactive power output [165]. Since, the P bus with unspecified reactive source injection, Q controls the voltage magnitude of remotely located PQV bus, hence this unknown quantity Q becomes the state variable, while real power generation at P bus is set to zero. A PQV bus has the characteristics of a PQ bus with known voltage magnitude in

addition to real and reactive power injections [165]. By injecting the appropriate amount of reactive power at P bus, the desired magnitude of voltage at PQV bus is achieved. The detailed explanation regarding concept of PQV and P buses has been illustrated by means of a simple 5 bus system shown in Figure 4.1. In Figure 4.1, bus 1 is set as a reference bus, buses 2 and 4 are assigned as PQ buses while buses 3 and 5 have been designated as P and PQV bus, respectively. To incorporate the concept of the P bus (bus 3) to keep the magnitude of voltage of the PQV bus (bus 5) constant, set of equations augmented are given by (4.1) and (4.2) as below:

$$\boldsymbol{\Delta V} = [\Delta V_2 \quad \Delta V_3 \quad \Delta V_4] \tag{4.1}$$

$$\boldsymbol{\Delta Q} = [\Delta Q_2 \quad \Delta Q_4 \quad \Delta Q_5] \tag{4.2}$$

With the above modification, equation augmented relating to power mismatch with respect to corrections in phase angles and voltage magnitudes for the Newton-Raphson algorithm takes the form as below:

$$\boldsymbol{Y} = \boldsymbol{JX} \tag{4.3}$$

where,

$$\boldsymbol{Y} = [\Delta P_2 \quad \Delta P_3 \quad \Delta P_4 \quad \Delta P_5 \quad \Delta Q_2 \quad \Delta Q_4 \quad \Delta Q_5]^T \tag{4.4}$$

$$\boldsymbol{X} = [\Delta \delta_2 \quad \Delta \delta_3 \quad \Delta \delta_4 \quad \Delta \delta_5 \quad \Delta V_2 \quad \Delta V_3 \quad \Delta V_4]^T \tag{4.5}$$

$$\boldsymbol{J} = \begin{bmatrix} \frac{\partial P_2}{\partial \delta_2} & \frac{\partial P_2}{\partial \delta_3} & \frac{\partial P_2}{\partial \delta_4} & \frac{\partial P_2}{\partial \delta_5} & \frac{\partial P_2}{\partial V_2} & \frac{\partial P_2}{\partial V_3} & \frac{\partial P_2}{\partial V_4} \\ \frac{\partial P_3}{\partial \delta_2} & \frac{\partial P_3}{\partial \delta_3} & \frac{\partial P_3}{\partial \delta_4} & \frac{\partial P_3}{\partial \delta_5} & \frac{\partial P_3}{\partial V_2} & \frac{\partial P_3}{\partial V_3} & \frac{\partial P_3}{\partial V_4} \\ \frac{\partial P_4}{\partial \delta_2} & \frac{\partial P_4}{\partial \delta_3} & \frac{\partial P_4}{\partial \delta_4} & \frac{\partial P_4}{\partial \delta_5} & \frac{\partial P_4}{\partial V_2} & \frac{\partial P_4}{\partial V_3} & \frac{\partial P_4}{\partial V_4} \\ \frac{\partial P_5}{\partial \delta_2} & \frac{\partial P_5}{\partial \delta_3} & \frac{\partial P_5}{\partial \delta_4} & \frac{\partial P_5}{\partial \delta_5} & \frac{\partial P_5}{\partial V_2} & \frac{\partial P_5}{\partial V_3} & \frac{\partial P_5}{\partial V_4} \\ \frac{\partial Q_2}{\partial \delta_2} & \frac{\partial Q_2}{\partial \delta_3} & \frac{\partial Q_2}{\partial \delta_4} & \frac{\partial Q_2}{\partial \delta_5} & \frac{\partial Q_2}{\partial V_2} & \frac{\partial Q_2}{\partial V_3} & \frac{\partial Q_2}{\partial V_4} \\ \frac{\partial Q_4}{\partial \delta_2} & \frac{\partial Q_4}{\partial \delta_3} & \frac{\partial Q_4}{\partial \delta_4} & \frac{\partial Q_4}{\partial \delta_5} & \frac{\partial Q_4}{\partial V_2} & \frac{\partial Q_4}{\partial V_3} & \frac{\partial Q_4}{\partial V_4} \\ \frac{\partial Q_5}{\partial \delta_2} & \frac{\partial Q_5}{\partial \delta_3} & \frac{\partial Q_5}{\partial \delta_4} & \frac{\partial Q_5}{\partial \delta_5} & \frac{\partial Q_5}{\partial V_2} & \frac{\partial Q_5}{\partial V_3} & \frac{\partial Q_5}{\partial V_4} \end{bmatrix}. \tag{4.6}$$

With the above modification in the NRLF equation, the correction vector defined by (4.5) is calculated using (4.3), and voltage magnitudes and angles are updated. The net reactive power injection (Q_3) at P bus 3 is calculated as per following:

$$Q_3 = -\mathrm{Im}\left[\overline{V}_3^* \sum_{j=1}^{5} \overline{y}_{3j}\overline{V}_j\right] \tag{4.7}$$

where, $\overline{V}_j$ represents complex voltage at bus j and $\overline{y}_{3j}$ corresponds to elements of bus admittance matrix.

To keep the voltage of PQV bus constant, different voltage controlling devices given in [166] may be utilized. In this work, the desired PQV bus voltage is achieved by assuming a shunt capacitor placed at P bus due to its low cost compared to other voltage controlling devices.

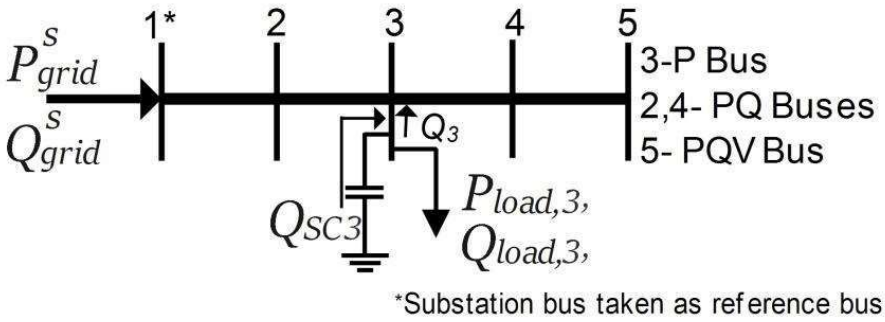

Figure 4.1: Simple 5 bus network with novel P, PQV bus pair

In Figure 4.1, Q_{SC} represents the amount of reactive power injection by the shunt capacitor placed at P bus 3 to maintain voltage of PQV bus 5 constant. Once, the net reactive power injection Q_3 at bus 3 is obtained using (4.7), the value of reactive power Q_{SC3} requisite at P bus 3 to keep the voltage magnitude constant at PQV bus 5 is computed using,

$$Q_{SC3} = Q_3 + Q_{load,3} \tag{4.8}$$

where, Q_3 = net reactive power injection at bus 3.

Q_{sc3} = reactive power injection by shunt capacitor at bus 3.

$Q_{load,3}$ = specified reactive power load at bus 3.

4.2.2 NRLF Equation under PQV and Q buses

Similarly, inclusion of Q, PQV bus pair in the system needs the Jacobian matrix to be modified for solving Newton Raphson load flow. Here, the voltage magnitude of the PQV bus is controlled by regulating the real power injection at Q bus. A Q bus is equipped with a controllable and unspecified real power source and fixed reactive power generation. The Q bus in general, is a generator bus with zero reactive power generation. Since the voltage magnitude of PQV bus is controlled remotely by varying real power injection at the Q bus, the real power associated with this Q bus remains unknown and needs to be solved as a state variable. The concept of Q and

PQV buses has been explained through a 5 bus system with bus 3 and 5 considered as Q and PQV bus, respectively. The single line diagram of the system is shown in Figure 4.2. Since the real power at Q bus is not known, hence ΔP_3 at Q bus 3 is removed from the mismatch vector. For the system having bus-3 as Q bus to control the voltage of PQV bus 5 the augmented set of equations for corrections and mismatches takes the form given by (4.1) and (4.9).

$$\boldsymbol{\Delta P} = [\Delta P_2 \quad \Delta P_4 \quad \Delta P_5] \tag{4.9}$$

With the above modification, equation augmented relating to power mismatch with respect to corrections in the phase angles and voltage magnitudes for the Newton-Raphson algorithm takes the form given by (4.3) with $\boldsymbol{X}$ given by (4.5) and $\boldsymbol{Y}$ given by,

$$\boldsymbol{Y} = [\Delta P_2 \quad \Delta P_4 \quad \Delta P_5 \quad \Delta Q_2 \quad \Delta Q_3 \quad \Delta Q_4 \quad \Delta Q_5]^T \tag{4.10}$$

$$\boldsymbol{J} = \begin{bmatrix} \frac{\partial P_2}{\partial \delta_2} & \frac{\partial P_2}{\partial \delta_3} & \frac{\partial P_2}{\partial \delta_4} & \frac{\partial P_2}{\partial \delta_5} & \frac{\partial P_2}{\partial V_2} & \frac{\partial P_2}{\partial V_3} & \frac{\partial P_2}{\partial V_4} \\ \frac{\partial P_4}{\partial \delta_2} & \frac{\partial P_4}{\partial \delta_3} & \frac{\partial P_4}{\partial \delta_4} & \frac{\partial P_4}{\partial \delta_5} & \frac{\partial P_4}{\partial V_2} & \frac{\partial P_4}{\partial V_3} & \frac{\partial P_4}{\partial V_4} \\ \frac{\partial P_5}{\partial \delta_2} & \frac{\partial P_5}{\partial \delta_3} & \frac{\partial P_5}{\partial \delta_4} & \frac{\partial P_5}{\partial \delta_5} & \frac{\partial P_5}{\partial V_2} & \frac{\partial P_5}{\partial V_3} & \frac{\partial P_5}{\partial V_4} \\ \frac{\partial Q_2}{\partial \delta_2} & \frac{\partial Q_2}{\partial \delta_3} & \frac{\partial Q_2}{\partial \delta_4} & \frac{\partial Q_2}{\partial \delta_5} & \frac{\partial Q_2}{\partial V_2} & \frac{\partial Q_2}{\partial V_3} & \frac{\partial Q_2}{\partial V_4} \\ \frac{\partial Q_3}{\partial \delta_2} & \frac{\partial Q_3}{\partial \delta_3} & \frac{\partial Q_3}{\partial \delta_4} & \frac{\partial Q_3}{\partial \delta_5} & \frac{\partial Q_3}{\partial V_2} & \frac{\partial Q_3}{\partial V_3} & \frac{\partial Q_3}{\partial V_4} \\ \frac{\partial Q_4}{\partial \delta_2} & \frac{\partial Q_4}{\partial \delta_3} & \frac{\partial Q_4}{\partial \delta_4} & \frac{\partial Q_4}{\partial \delta_5} & \frac{\partial Q_4}{\partial V_2} & \frac{\partial Q_4}{\partial V_3} & \frac{\partial Q_4}{\partial V_4} \\ \frac{\partial Q_5}{\partial \delta_2} & \frac{\partial Q_5}{\partial \delta_3} & \frac{\partial Q_5}{\partial \delta_4} & \frac{\partial Q_5}{\partial \delta_5} & \frac{\partial Q_5}{\partial V_2} & \frac{\partial Q_5}{\partial V_3} & \frac{\partial Q_5}{\partial V_4} \end{bmatrix} \tag{4.11}$$

With the above modification in the NRLF equation, unknown voltage magnitudes and angles are calculated to find real power injection at Q bus 3 as per following:

$$P_3 = \mathrm{Re}\left[\overline{V}_3^* \sum_{j=1}^{5} \overline{y}_{3j}\overline{V}_j\right] \tag{4.12}$$

In this work, the voltage of PQV bus is controlled by assuming a dispatchable DG placed at Q bus to inject variable real power.

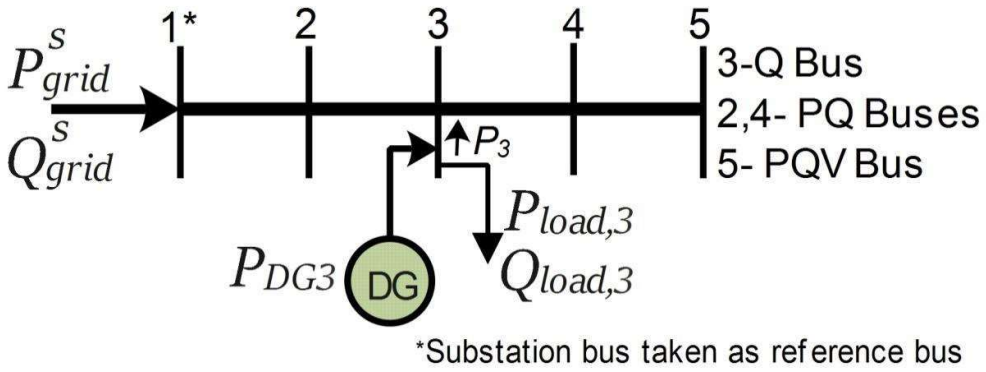

Figure 4.2: Five bus network with novel Q, PQV bus pair.

In Figure 4.2, P_{DG3} represents the amount of real power injected by the dispatchable DG placed at Q bus 3 to maintain voltage of PQV bus 5 constant. Once, the net real power injection P_3 at bus 3 is obtained using (4.12), the value of real power P_{DG3} requisite at Q bus 3 to keep the voltage magnitude at PQV bus 5 constant is computed using (4.13).

$$P_{DG3} = P_3 + P_{load,3} \tag{4.13}$$

where, P_3 = net real power injection at bus-3.

P_{DG3} = real power injection by DG at bus-3.

$P_{load,3}$ = specified real power load at bus-3.

4.3 PROBLEM FORMULATION: OBJECTIVE FUNCTION AND CONSTRAINTS

Present work has considered minimization of multi-objective function given by (3.9) for the reconfigured distribution network under DG placement in the presence of P/Q and PQV buses. Also, a new multi-objective function is proposed in this chapter that has also been minimised for the reconfigured distribution network under DG placement in the presence of P/Q and PQV buses. Results obtained on two multi-objective functions (i.e. multi-objective function proposed in chapter 3 that has been given by (3.9) and new multi-objective function proposed in this chapter) have been compared. The optimization has been performed using modified grey wolf optimization approach. The new multi-objective function is formulated below.

4.3.1 Proposed new multi-objective function

Deficiency in reactive power supplied is one of the major causes for voltage instability that restricts the varying load growth to be operated within the stable region. In case of reactive power deficiency, it may not be possible to maintain all bus voltages close to desired flat values. So, it would be desirable to serve as large amount of load as possible at the enhanced voltage level. Voltage profile improvement index VPI is an index that considers the bus voltage level, but it cannot discriminate the buses with lightly loaded and heavily loaded conditions. Therefore, the index QLI given by (3.18) and (3.19) has been considered in this work to maximize voltage stability margin. This index takes into account the power consumed by each load and voltage level. The objective function to maximize voltage stability margin is given as:

$$f_3 = \text{maximize}\, QLI = \sum_{i=1}^{nb} [P_{load,i} V_i] \tag{4.14}$$

where, $P_{load,i}$ and V_i are the the real power demand and voltage magnitude at bus-i.

Real power loss minimization has been considered using objective function given by (3.6) in chapter 3. Since, the two objectives are different in nature, they have been combined to take the form of single objective function by converting the maximization function into minimization. Proposed new multi-objective function considers minimization of real power loss in the network and ensures loadability enhancement by supply of maximum amount of quality load to the consumers at enhanced voltage magnitude. The proposed new multi-objective function is given as:

$$\text{minimize}\, g = w_1 f_1 - w_3 f_3 \tag{4.15}$$

$$\text{subjected to}\, w_1 + w_3 = 1 \tag{4.16}$$

where, w_1 and w_3 represents weight assigned to f_1 and f_3, respectively. The new index considers both the real power loss reduction and quality load to be enhanced to increase voltage stability margin. To convert the maximization optimization formulation into minimization, negative sign has been assigned to the objective function, f_3. The multi-objective function given by (3.9) as well as new multi-objective function given by (4.15) have been minimized under network reconfiguration and DG placement in the presence of P/Q and PQV buses with set of equality and inequality constraints defined in Section 2.5.2 (chapter 2) and Section 2.5.3 (chapter 2), respectively and radiality constraint given by (3.4) and (3.5) in chapter 3, satisfied.

4.4 PROPOSED GWO BASED ALGORITHM FOR MULTI-OBJECTIVE FUNCTION

The modified GWO is performed under set of decision variables and population matrix defined by (3.3) and (3.11)–(3.13) presented in chapter 3.

The flowchart for proposed GWO based stability enhancement and loss minimization approach under optimal DG placement, network reconfiguration in the presence of PQV and P/Q buses is shown in Figure 4.3. As per this flowchart, maximum loadability of the system is computed under optimal fitness function and decision variables, where decision variables consist of open status of tie switches and DG location and size. The calculation method for maximum loadability is presented in Section 3.5 in Chapter 3.

Apart from base case, the following cases have been studied to examine impact of DG allocation, network reconfiguration and presence of PQV and P/Q buses in voltage stability margin (maximum loadability) enhancement and loss reduction.

Cases under study:

Case 4: P/Q, PQV buses allocation for base case system.

Case 5: Reconfiguration with P/Q, PQV buses.

Case 6: Reconfiguration & Type-1 DG allocation with P/Q, PQV buses.

Case 7: Reconfiguration & Type-3 DG (0.82 pf) allocation with P/Q, PQV buses.

Case 8: Reconfiguration & Type-3 DG (0.9 pf) allocation with P/Q, PQV buses.

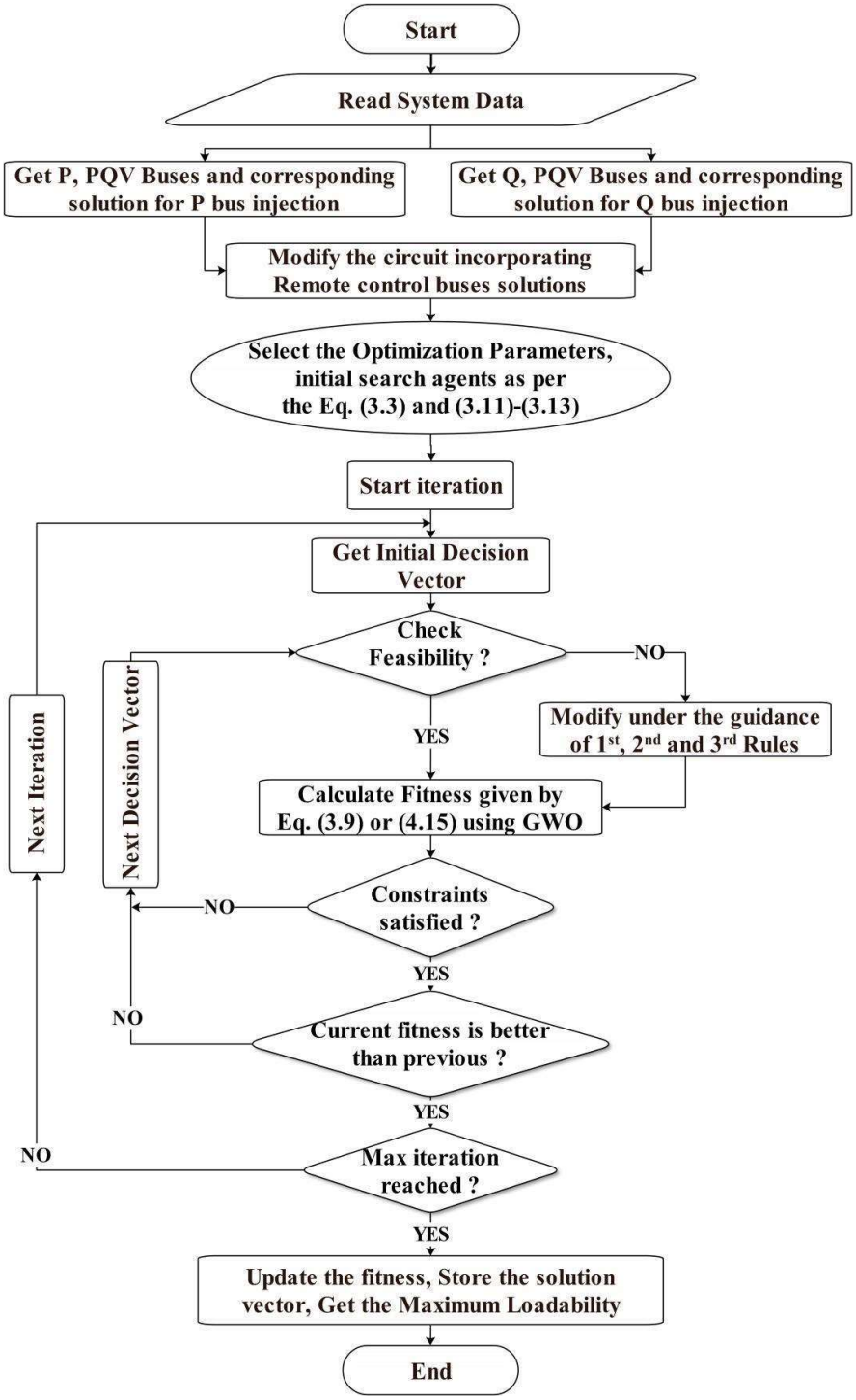

Figure 4.3: Flowchart for minimization of multi-objective fitness function using modified GWO algorithm

4.5 RESULTS AND DISCUSSION

To validate the effectiveness of the proposed algorithm, numerical simulation is accomplished on IEEE 33-bus [126] and 69-bus reconfigurable distribution systems. The 33-bus test system consists of 37 branches including tie-lines. It has bus-1 as substation bus or reference bus and all other buses are PQ load buses. The 33-bus test system consists of 32 generally closed branches and 5 tie-switches generally kept open with 4 feeders. The total load demand on substation bus of this RDS constitutes of 3.715 MW real and 2.3 MVAr reactive power load. The 69-bus test system consists of a total of 73 branches including all the tie-lines. It has bus-1 as substation bus or reference bus and all other buses are PQ load buses. The 69-bus test system consists of 68 generally closed branches and 5 tie-switches generally kept open with 7 feeders. The total load demand on substation bus of this RDS constitutes 3.802 MW of real and 2.694 MVAr reactive power. The details of these two systems are given in appendix A and B, respectively. The simulation study is performed using code developed on MATLAB on a system having Intel(R) Core(TM) i7-8700 CPU @ 3.20 GHz processor. The results obtained on the two test systems are presented below:

4.5.1 Test system 1 (33-bus RDS)

4.5.1.1 *Selection of PQV bus*

The PQV bus was selected based on a criterion of being farthest bus having lowest voltage magnitude. Base case voltage magnitudes of all the buses have been shown in Table 4.1. It is observed from Table 4.1 that remote bus 18 has got a voltage magnitude of 0.9131 pu, which is lowest. Therefore, bus 18 was selected as PQV bus for 33-bus radial distribution system. The pre-defined voltage of PQV bus (bus

18) was set as 0.93 pu for the base case condition. The enhanced voltage was to be obtained through reactive power injection at P bus or real power injection at Q bus.

Table 4.1: Base case voltage magnitude at buses (33-bus RDS)

Bus No.	Voltage magnitude (pu)	Bus No.	Voltage magnitude (pu)	Bus No.	Voltage magnitude (pu)
1	1	12	0.9269	23	0.9794
2	0.9970	13	0.9208	24	0.9727
3	0.9829	14	0.9185	25	0.9694
4	0.9755	15	0.9171	26	0.9477
5	0.9681	16	0.9157	27	0.9452
6	0.9497	17	0.9137	28	0.9337
7	0.9462	**18**	**0.9131**	29	0.9255
8	0.9413	19	0.9965	30	0.9220
9	0.9351	20	0.9929	31	0.9178
10	0.9292	21	0.9922	32	0.9169
11	0.9284	22	0.9916	33	0.9166

4.5.1.2 *Results considering PQV and P buses*

4.5.1.2.(i) Considering multi-objective function proposed in chapter 3

As the primary objective of the work is to enhance the maximum loadability of the RDS and to lower the active power loss, a suitable designation of P bus should be accomplished, accordingly. To designate a P bus, all the buses (except reference bus) on the feeder connected to PQV bus 18 (minimum voltage bus) are chosen as candidate buses for P bus selection. Each and every bus on this feeder except bus-18 itself are analysed to designate P bus for the maximum voltage stability margin (maximum loadability) and least active power loss. In order to select P bus, a shunt capacitor is connected at a bus and its reactive power output is determined along-with VSI_{min}, maximum loadability (λ_{max}) and active power loss (APL) of the system. The procedure is repeated for other buses. The reactive power injection by shunt capacitor, maximum loadability (λ_{max}), voltage stability index at the

maximum loadability point VSI_{min} and active power loss (APL) values under shunt capacitor connection at each bus have been shown in Table 4.2.

Table 4.2: P Bus selection for 33-bus RDS

Bus No.	**Shunt Capacitor Injection (MVAr)**	**λ_{max}**	**VSI_{min}**	**APL (kW)**	**Bus No.**	**Shunt Capacitor Injection (MVAr)**	**λ_{max}**	**VSI_{min}**	**APL (kW)**
2	54.71986	2.74	0.75206	1727.1	10	0.659	2.73	0.72612	172.6
3	8.48739	2.75	0.75214	322.06	11	0.6478	2.73	0.72577	172.93
4	5.18178	2.76	0.75211	233.62	12	0.6274	2.73	0.72515	173.6
5	3.66845	2.77	0.75212	194.36	13	0.4846	2.72	0.72084	177.56
6	**1.75353**	**2.78**	**0.7580**	**154.44**	14	0.4248	2.72	0.71905	179.39
7	1.21536	2.75	0.74346	159.37	15	0.390	2.71	0.71799	180.86
8	1.09045	2.75	0.73947	162.90	16	0.3595	2.71	0.71705	182.29
9	0.82219	2.74	0.7311	168.86	17	0.2881	2.69	0.71489	185.37

VS_{min} = VSI at maximum loadability point

It is observed from Table 4.2 that connection of shunt capacitor at bus 6 offers the highest maximum loadability, highest voltage stability index, and lowest real power loss compared to other buses under consideration. Therefore bus-6 is selected and assigned as the P bus with shunt capacitor injecting 1.75353 MVAr of reactive power. Real and reactive power loss, maximum loadability (λ_{max}) and voltage stability index obtained at the nose point (VSI_{min}) have been shown in Table 4.3 in the absence of P, PQV buses and in the presence of P, PQV buses. A significant enhancement of 5.71% has been achieved for maximum system loadability, and significant reduction of 23.80% and 22.18%, respectively have been achieved in real and reactive power loss, respectively, under selected pair of P bus (bus 6) and PQV bus (bus 18).

Table 4.3: Results before and after selection of P, PQV buses in the IEEE 33-bus RDS

Description	**Q_{sh} @ P bus**	**APL (kW)**	**QPL (kVAr)**	**λ_{max}**	**VSI_{min}**	**V_{min} (pu) & V_{max} (pu)**
Base Case Results (with only PQ buses)	-----	202.68	135.14	2.63	0.6951	V_{min} = 0.9131 @ 18 V_{max} = 1.0 @ 1
Base Case Results (with P, PQV buses)	1.75353 MVAr @6	154.44	105.16	2.78	0.7580	V_{min} = 0.93 @ 18 V_{max} = 1.0 @ 1

Table 4.3 demonstrates the active power loss, loadability, maximum and minimum voltage of the test system before and after the selection of PQV and P bus in the 33-bus system. It shows that suitably allocating the P bus in the original system not only maintains the desired voltage level of 0.93 pu at the PQV bus but also enhances the performance of overall system in terms of maximum loadability, improved voltage stability index, minimum losses, and improved voltage profile.

Table 4.4 demonstrates the outcomes of the IEEE 33-bus RDS for the various cases studied with incorporation of the PQV and P buses by considering the multi-objective function proposed in chapter 3. Incorporating P, PQV buses, followed by network reconfiguration by opening the switches associated with set of lines (7, 9, 14, 32, 37) the real power loss drops from 154.44 kW to 118.15 kW, while loadability of the system increases to 4.08 pu. The minimum voltage of the network has improved to 0.9477 pu at bus-33 which is above the set target of 0.93 pu. Further, the application of simultaneous reconfiguration and Type-1 DG (injecting only real power of 3.651093 MW at bus-6) allocation enhances the loadability of the system to 5.59 pu while keeping the active power losses to a minimum of 69.2 kW, thus improving the loadability by 112.54% while the losses are reduced by 65.86%. In this case the system minimum voltage magnitude have further enhanced to 0.9850 pu at bus-32.

Further investigations have been carried out with Type-3 DG placed in the system injecting both real and reactive power operating at 0.82 and 0.90 power factors, respectively as Case 4 and Case 5, respectively. For Case 4, considering the network reconfiguration and Type-3 DG at 0.82 power factor, the optimal solution has been found as DG of 2.53622 MVA placed at bus-9 and opening the switches associated with set of lines (6, 14, 21, 30, 37) increases the system maximum loadability by 161.98% to 6.89, while reducing the real power loss to 86.03 kW and reactive power loss to 67.47 kVAr. The minimum system voltage has been improved to 0.9790 pu at bus-30. All other indicators for performance have been enhanced. Similarly, for Case 5, placing a DG of 2.99695 MVA at 0.90 power factor and opening the switches associated with set of lines (14, 20, 32, 35, 37) increases the maximum system loadability by 132.70% to 6.12, while reducing the real and reactive power losses by 58.80% and 53.71% to 83.49 kW and 62.55 kVAr, respectively.

Table 4.4: Results after P and PQV bus consideration for 33-bus RDS

Items	**Results with Multi-objective function in chapter 3**				
	Case 1	**Case 2**	**Case 3**	**Case 4**	**Case 5**
Open switches	33, 34, 35, 36, 37	7, 9, 14, 32, 37	14, 20, 32, 35, 37	6, 14, 21, 30, 37	14, 20, 32, 35, 37
DG MW @ bus	----	----	3.65109 @ 6	2.53622 @ 9	2.99694 @ 8
APL (kW)	154.44	118.15	69.2	86.03	83.49
QPL (kVAr)	105.16	89.85	55.48	67.47	62.55
λ_{max}	2.78	4.08	5.59	6.89	6.12
NVVB	14	3	0	0	0
VDI	0.00914	0.00055	0	0	0
VPI	0.0060	0.0272	0.0982	0.3939	0.3698
QLI/QLI$_m$	3.5703	3.6073	3.6932	3.7186	3.7140
APLR%	23.80	41.71	65.86	57.55	58.81
QPLR%	22.18	33.51	58.95	50.07	53.72
V_{min} @ bus	0.93 @18	0.9477 @ 33	0.9850 @ 32	0.9790 @ 30	0.9833 @ 32
V_{max} @ bus	1 @ 1	1 @ 1	1.013 @ 6	1.03 @ 9	1.02@ 8

Figures are drawn for the maximum system loadability, voltage profile, system loss and voltage stability indices for all the cases under study as Figure 4.4, Figure 4.5, Figure 4.6 and Figure 4.7, respectively. Figure 4.4 shows that the highest maximum system loadability is achieved by implementation of Case 4. Figure 4.5 presents voltage profile of all the cases, which shows that voltage magnitudes are lying well within the permissible limits except Case 1 and Case 2. Consequently, Case 4 awards a considerable enhancement in the performance indices and harvests best maximum loadability at highest voltage profile improvement. The proposed multi-objective algorithm for enhancement of maximum system loadability increases the network loadability with considerable reduction in active power loss, with all buses within the specified voltage limits except Case 2.

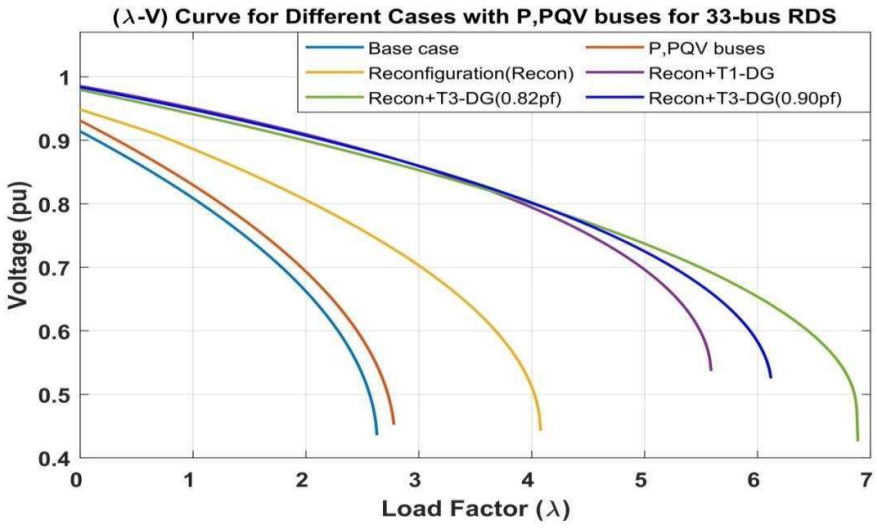

Figure 4.4: Loadability curve of cases with P, PQV buses for IEEE 33-bus RDS

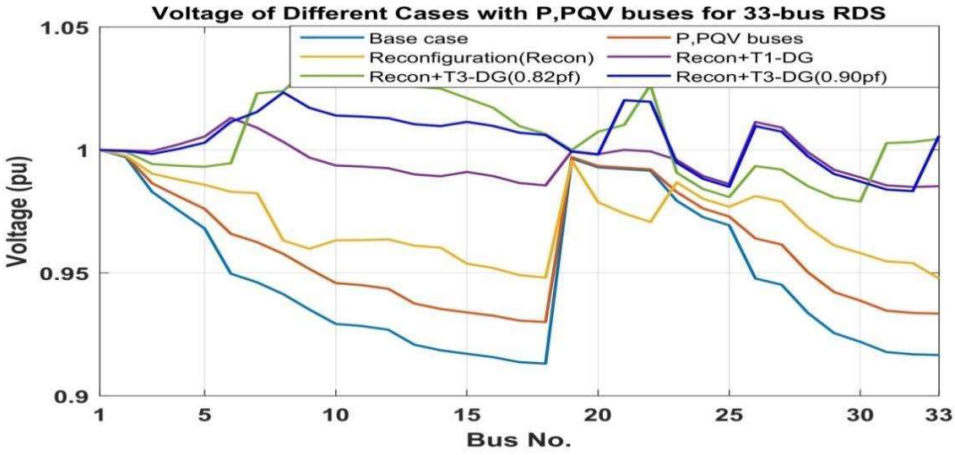

Figure 4.5: Voltage profile of cases with P, PQV buses for IEEE 33-bus RDS

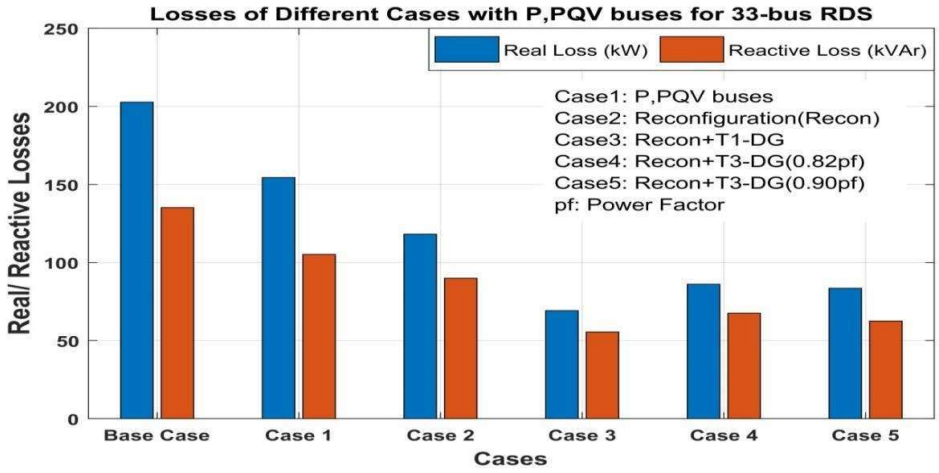

Figure 4.6: System Losses of cases with P, PQV buses for IEEE 33-bus RDS

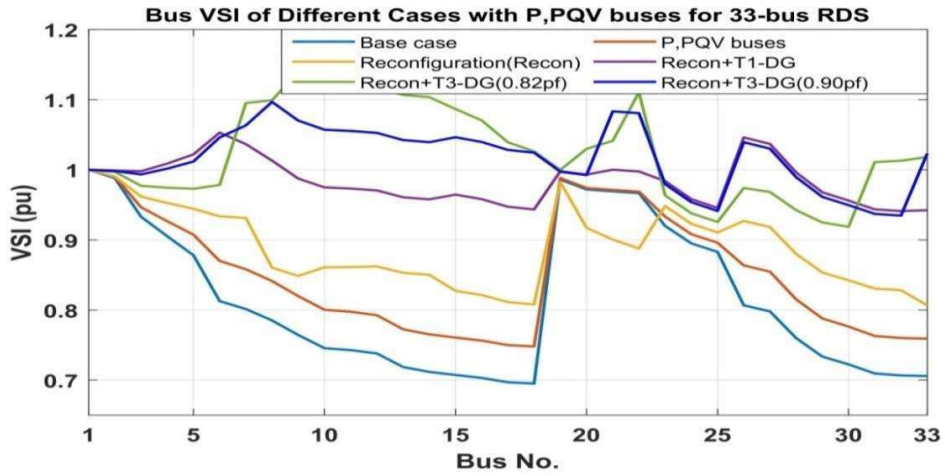

Figure 4.7: VSI of cases with P, PQV buses for IEEE 33-bus RDS

4.5.1.2.(ii) Considering new multi-objective function proposed in this chapter

For selection of a P bus, the optimization procedure is performed with connection of shunt capacitor at each bus considered at a time. The bus with minimum value of fitness function defined by equation (4.15) is selected as P bus. The objective function considers both reduction in real power loss and enhancements in load quality to be served that ultimately enhance the maximum system loadability. Figure 4.8, shows the real and reactive power loss of the system, QLI and reactive power injected through shunt capacitor connected at the bus under consideration as P bus. In Figure 4.8, results are presented for every possible bus to be assigned as P bus to keep the desired voltage level of 0.93 pu at PQV bus-18. It is observed that consideration of bus-29 as P bus minimizes the multi-objective function with minimum real power loss and enhanced QLI with higher maximum loadability. Therefore, bus-29 is selected and assigned as the P bus with shunt capacitor injecting 1.74646 MVAr of reactive power as shown in Table 4.5. Table 4.5 also shows real and reactive power loss, maximum loadability, minimum voltage stability index (VS_{min}) and minimum and maximum voltage in absence of P, PQV buses as well as in presence of P, PQV buses. It is observed from Table 4.5 that choosing bus-29 as P bus yields maximum system loadability and real and reactive power loss of the system as 2.95, 151.25 kW and 102.81 kVAr, respectively, and minimum value of VSI as 0.7580. A significant enhancement of 12.17% has been achieved in maximum system loadability and a significant reduction of 25.38% and 23.92%, respectively have been obtained in real and reactive power loss, respectively with the incorporation of selected P, PQV buses in the system.

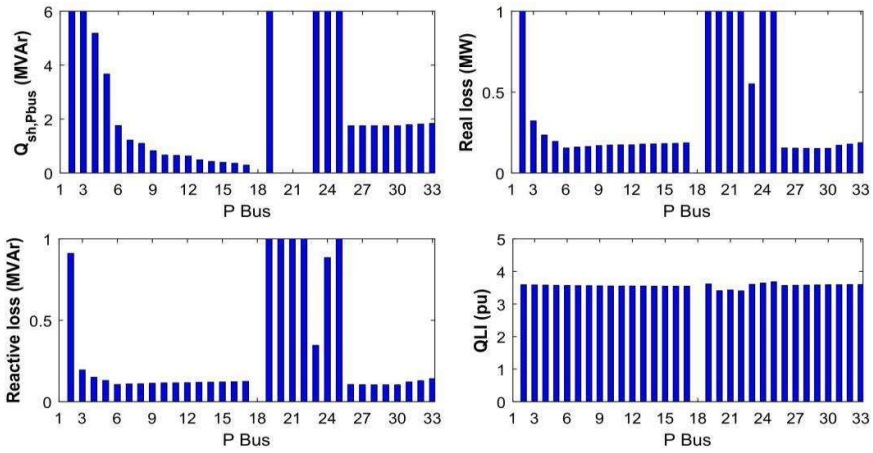

Figure 4.8: P bus selection Criterian for IEEE 33-bus RDS

Table 4.5: Results before and after selection of P, PQV buses in the IEEE 33-bus RDS

Description	**Q_{sh} @ P bus**	**APL (kW)**	**QPL (kVAr)**	**λ_{max}**	**VSI_{min}**	**V_{min} (pu) & V_{max} (pu)**
Base Case Results (with only PQ buses)	-----	202.68	135.14	2.63	0.6951	V_{min} = 0.9131 @ 18 V_{max} = 1.0 @ 1
Base Case Results (with P, PQV buses)	1.74646 MVAr @ 29	151.25	102.81	2.95	0.7580	V_{min} = 0.93 @ 18 V_{max} = 1.0 @ 1

Table 4.6 presents different performance indices for the five cases considered of the 33-bus system incorporating P, PQV buses by proposed method. Incorporating P, PQV buses, followed by network reconfiguration by opening the switches associated with set of lines (7, 9, 14, 28, 32), the real power loss drops from 151.25 kW to 109.55 kW, while loadability of the system increases to 4.75 pu. The minimum voltage of the network has improved to 0.9477 pu at bus-33 which is above the set target value of 0.93 pu. Further, the application of simultaneous reconfiguration and Type-1 DG (injecting only real power of 1.94446 MW operating at unity power factor) allocation at bus-25 enhances the loadability of the system to 6.93 pu while keeping the active power loss to a minimum of 49.27 kW, thus improves the loadability by 163.5% while the loss is reduced by 75.69%. In this case the system minimum voltage magnitude has further enhanced to 0.9644 pu at bus-17.

As shown in Table 4.6, further investigations have been carried out under Type-3 DG in the system injecting both real and reactive power operating at 0.82 power factor (Case 4), and 0.90 power factor (Case 5), respectively. For Case 4, considering the network reconfiguration and Type-3 DG at 0.82 power factor, the optimal solution has been found as DG of 2.80449 MVA placed at bus-9 and opening the switches associated with set of lines (14, 20, 28, 32, 35) increases the system maximum loadability by 175.67% to 7.25, while reducing the real power loss to 84.45 kW and reactive power loss to 65.58 kVAr. The minimum system voltage has been improved to 0.9909 pu at bus-25. All other indicators for performance have been enhanced. Similarly, for Case 5, placing a DG of 3.0190 MVA at 0.90 power factor and opening the switches associated with set of lines (14, 20, 32, 35, 37) increases the maximum system loadability by 153.61% to 6.67, while reducing the real and reactive power losses by 61.85% and 54.90% to 77.32 kW and 60.95 kVAr, respectively.

Table 4.6: Results after P and PQV bus consideration for IEEE 33-bus RDS

Items	**Results with new multi-objective function**				
	Case 1	**Case 2**	**Case 3**	**Case 4**	**Case 5**
Open switches	33, 34, 35, 36, 37	7, 9, 14, 28, 32	7, 9, 14, 17, 28	14, 20, 28, 30, 35	14, 20, 32, 35, 37
DG MW @ bus	---	---	1.94446 @ 25	2.80449 @ 9	3.0190 @ 7
APL (kW)	**151.25**	**109.55**	**49.27**	**84.45**	**77.32**
QPL (kVAr)	102.81	84.95	42.79	65.58	60.95
λ_{max}	**2.95**	**4.75**	**6.93**	**7.25**	**6.67**
NVVB	9	3	0	0	0
VDI	0.0074	0.000544	0	0	0
VPI	0.1128	0.18663	0.27239	0.3762	0.35306
QLI/QLI$_m$	3.5874	3.61982	3.68286	3.7184	3.7147
APLR%	25.38	45.948	75.688	58.33	61.85
QPLR%	23.92	37.132	68.330	51.47	54.90
V_{min} @ bus	0.9300 @ 18	0.9477 @ 33	0.9644 @ 17	0.9909 @ 25	0.9851 @ 25
V_{max} @ bus	1 @ 1	1 @ 1	1.008 @ 25	1.025@6	1.015 @ 7

Figure 4.9, Figure 4.10, Figure 4.11 and Figure 4.12 are drawn for the maximum system loadability, voltage profile, system loss and voltage stability indices, respectively, for all the cases under study. Figure 4.9 shows that the highest maximum system loadability is achieved by implementation of Case 4. Figure 4.10 presents voltage profile of all the cases, which shows that voltage magnitudes are lying well within the permissible limits except Case 1 and Case 2. Figure 4.11 shows the real and reactive power loss profile for different cases under study. From Figure 4.11 it can be observed that system loss is lowest for Case 3 compared to other cases. Figure 4.12 presents voltage stability indices of the system buses for all the cases from which it can be observed that minimum VSI is highest for Case 4 compared to other cases. Consequently, Case 4 awards a considerable enhancement in the performance indices and harvests best maximum loadability at highest voltage profile improvement. The proposed multi-objective algorithm for enhancement of maximum system loadability increases the network loadability with considerable reduction in active power loss, with all buses within the specified voltage limits except Case 2.

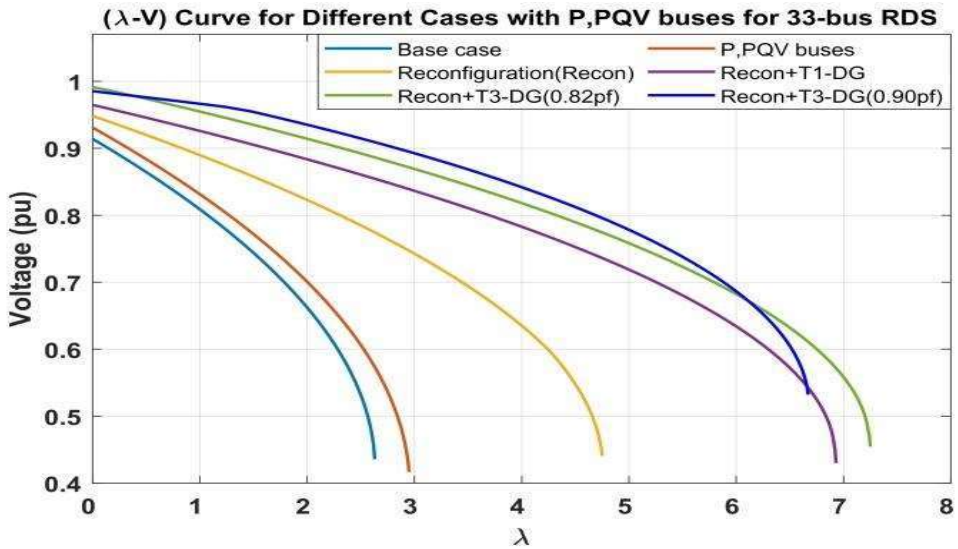

Figure 4.9: Loadability curve of cases with P, PQV buses for IEEE 33-bus RDS

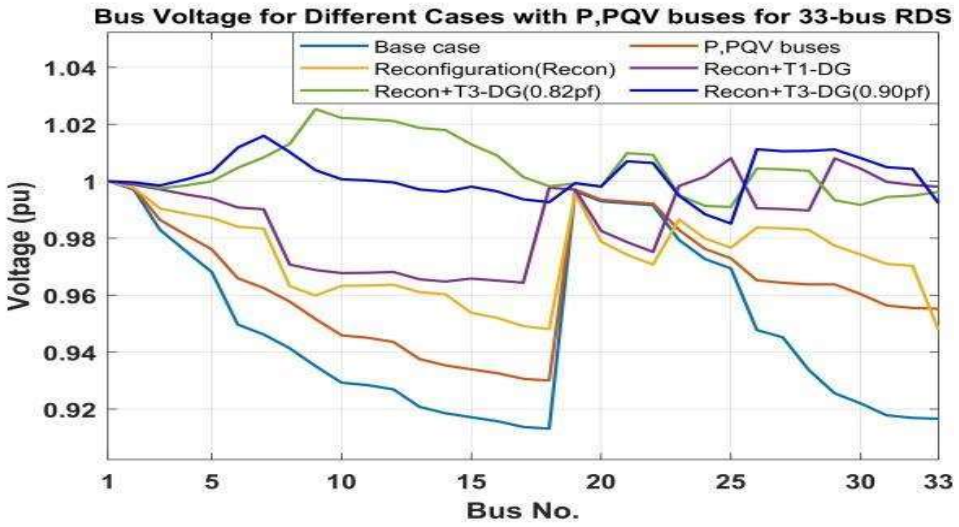

Figure 4.10: Voltage Profile of cases with P, PQV buses for IEEE 33-bus RDS

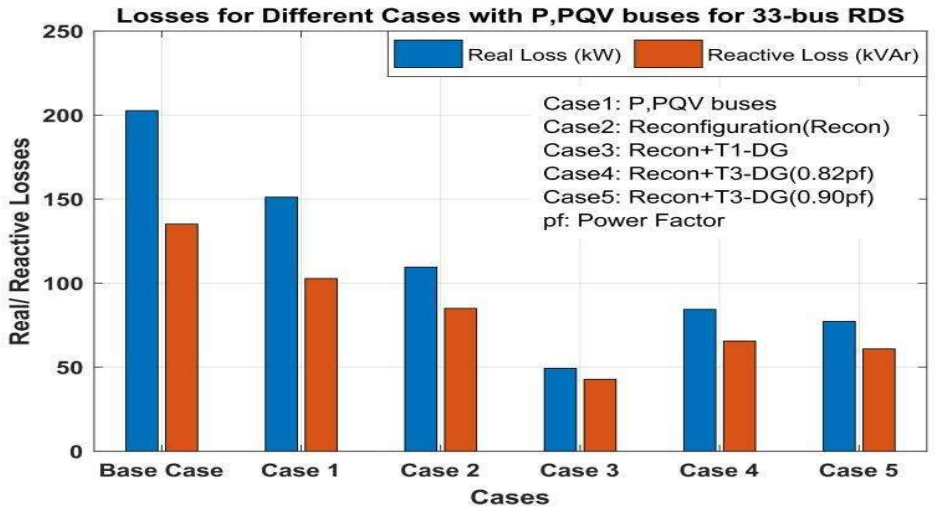

Figure 4.11: System Losses of cases with P, PQV buses for IEEE 33-bus RDS

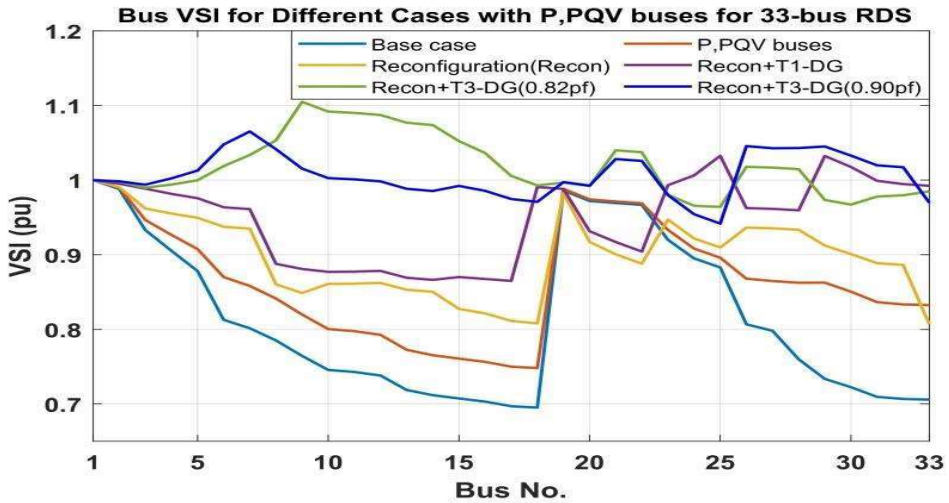

Figure 4.12: VSI of cases with P, PQV buses for IEEE 33-bus RDS

4.5.1.2.(iii) Comparison of results of two multi-objective functions

Table 4.7: Comparison of results for different cases with P,PQV buses for IEEE 33-bus RDS

Method/Case		Open switches	DG size @ bus	APL (kW)	λ_{max}	V_{min} @ bus
Only Reconfiguration (Case 2)	New multi-objective function	**7, 9, 14, 28, 32**	**NA**	**109.55**	**4.75**	**0.9477 @ 33**
	Multi-objective function (chapter 3)	7, 9, 14, 32, 37	NA	118.15	4.08	0.9477 @ 33
Reconfiguration and Type-1 DG (Case 3)	New multi-objective function	**7, 9, 14, 17, 28**	**1.94445 MW @ 25**	**49.27**	**6.93**	**0.9644 @ 17**
	Multi-objective function (chapter 3)	14, 20, 32, 35, 37	3.6510 MW @ 6	69.2	5.59	0.9849 @ 32
Reconfiguration and Type-3 DG (Case 4)	New multi-objective function	**14, 20, 28, 30, 35**	**2.80449 MVA @ 9**	**84.45**	**7.25**	**0.9909 @ 25**
	Multi-objective function (chapter 3)	6, 14, 21, 30, 37	2.53622 MVA @ 9	86.03	6.89	0.9790 @ 30
Reconfiguration and Type-3 DG (Case 5)	New multi-objective function	**14, 20, 32, 35, 37**	**3.0190 MVA @ 7**	**77.32**	**6.67**	**0.9851 @ 25**
	Multi-objective function (chapter 3)	14, 20, 32, 35, 37	2.99694 MVA @ 8	83.49	6.12	0.9833 @ 32

Table 4.7 presents the comparison of results obtained by multi-objective function proposed in this chapter with multi-objective function in chapter 3 for enhancing system performances under P, PQV buses. The Table 4.7 shows that system performances have been greatly enhanced in terms of loss reduction and maximum system loadability enhancement with the proposed multi-objective function in this chapter compared to multi-objective function proposed in chapter 3. The method

proposed in this chapter results in a better improvement in terms of real power loss reduction as well as maximum system loadability enhancement as compared to method with objective function proposed in Chapter 3 for P, PQV bus allocation under different cases as observed from Table 4.7.

4.5.1.3 *Results with PQV and Q buses considering new multi-objective function proposed in this chapter*

For selection of a Q bus, the optimization procedure is performed with dispatchable Type-1 DG connected at each bus considered at a time using the fitness function defined by (4.15). The bus with minimum value of fitness function defined by (4.15) is selected as Q bus. The objective fitness function considers both reduction in real power loss and enhancement in load quality to be served that ultimately enhances the maximum system loadability. Figure 4.13 shows the real and reactive power loss of the system, QLI and real power injected through DG connected at the bus under consideration as Q bus. In Figure 4.13, results are presented for every possible bus to be assigned as Q bus to keep the desired voltage level of 0.93 pu at PQV bus 18. It is observed that consideration of bus-30 as Q bus minimizes the multi-objective function with minimum real power loss and enhanced QLI with higher maximum loadability. Therefore, bus-30 is selected and assigned as the Q bus with DG injecting 1.101042 MW of real power, as shown in Table 4.8. Table 4.8 also shows real and reactive power loss, maximum loadability (λ_{max}), minimum voltage stability index (VS_{min}) and minimum and maximum voltage in the absence of Q, PQV buses as well as in presence of Q, PQV buses. It is observed from Table 4.8 that choosing bus-30 as Q bus yields maximum system loadability, and reduced real and reactive power loss of the system as 2.91, 123.94 kW and 84.65 kVAr, respectively, and minimum value of VSI as 0.7580. A significant enhancement of

10.65% has been achieved in maximum system loadability and a significant reduction of 38.85% and 37.36%, respectively have been obtained in real and reactive power loss, respectively, with the incorporation of selected Q, PQV pair of buses in the system.

Table 4.8: Results before and after selection of Q, PQV buses in the IEEE 33-bus RDS

Description	**P_{DG} @ Q bus**	**APL (kW)**	**QPL (kVAr)**	**λ_{max}**	**VSI_{min}**	**V_{min} (pu) & V_{max} (pu)**
Base Case Results (with only PQ buses)	---	202.68	135.14	2.63	0.6951	V_{min} = 0.9131 @ 18 V_{max} = 1.0 @ 1
Base Case Results (with Q, PQV buses)	1.101042 MW @ 30	123.95	84.65	2.91	0.7580	V_{min} = 0.93 @ 18 V_{max} = 1.0 @1

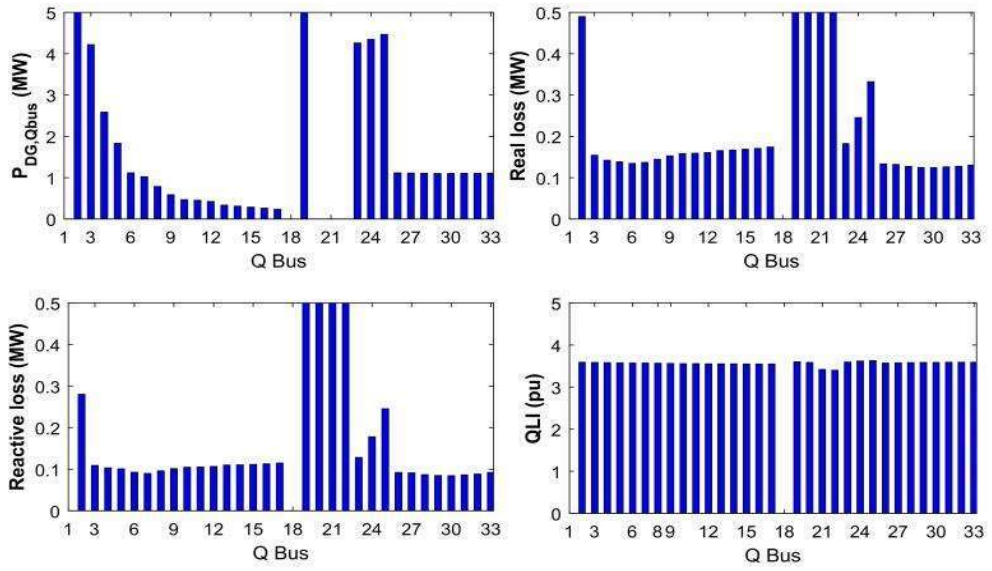

Figure 4.13: Q bus selection criterion for IEEE 33-bus RDS

Table 4.9, presents the performance indices of five cases considered for the 33-bus system incorporating Q, PQV buses by proposed method. Incorporating Q, PQV buses, followed by network reconfiguration by opening the switches associated with set of lines (7, 9, 14, 28, 32), the real power loss drops from 151.25 kW to 91.69 kW, while maximum loadability of the system increases to 4.69 pu. The minimum voltage of the

network has improved to 0.9477 pu at bus-33 which is above the set target value of 0.93 pu. Further, the application of simultaneous reconfiguration and Type-1 DG (1.05647 MW at bus-14) allocation enhances the loadability of the system to 6.26 pu while reducing the active power loss to a value of 64.95 kW, thus improving the loadability by 138.02% while the real power loss is reduced by 67.95%. In this case, the voltage has further enhanced to 0.9617 pu at bus-32.

As presented in Table 4.9, further investigations have been carried out for Type-3 DG injecting both real and reactive power at 0.82 power factor (Case 4) and 0.90 power factor (Case 5), respectively, while reconfiguring the network, simultaneously. For Case 4, considering the network reconfiguration and Type-3 DG at 0.82 power factor, the optimal solution has been reported as DG of 2.40518 MVA placed at bus-25 and opening the switches associated with set of lines (7, 10, 13, 15, 25), and it increases the system maximum loadability by 184.41% to 7.48 while reducing the network real and reactive power loss to 55.87 kW and 47.59 kVAr, respectively. The minimum system voltage has been improved to 0.9650 at bus-14 which is above the set target value of 0.93 pu. All other indicators for performance have also been enhanced. Similarly, for Case 5, placing a DG of 3.13818 MVA at bus-7 with 0.90 power factor and opening the switches associated with set of lines (12, 20, 32, 35, 37) increases the maximum system loadability by 149.81% to 6.57, while reducing the real and reactive power losses to 74.38 kW and 60.56 kVAr, respectively. With Case 5 into consideration, the network real and reactive power losses have been reduced by 63.30% and 55.18%, respectively. The Case 4 proves to be a highly favourable solution as it enhances the system performances mostly compared to all other cases under study, considering Q, PQV pair of buses for 33-bus reconfigurable test system.

Table 4.9: Results after Q, PQV buses consideration for IEEE 33-bus RDS

Items	Results with new multi-objective function				
	Case 1	**Case 2**	**Case 3**	**Case 4**	**Case 5**
Open switches	33, 34, 35, 36, 37	7, 9, 14, 28, 32	7, 8, 27, 31, 34	7, 10, 13, 15, 25	12, 20, 32, 35, 37
DG MW/ MVA @ bus	----	----	1.05647 @ 14	2.40518 @ 25	3.13818 @ 7
APL (kW)	**123.94**	**91.69**	**64.95**	**55.87**	**74.38**
QPL (kVAr)	84.65	72.39	50.18	47.59	60.56
λ_{max}	**2.91**	**4.69**	**6.26**	**7.48**	**6.57**
NVVB	9	3	0	0	0
VDI	0.00737	0.00050	0	0	0
VPI	0.11021	0.18602	0.22924	0.3247	0.35567
QLI/QLI$_m$	3.5876	3.61831	3.64292	3.7097	3.71795
APLR%	38.85	54.76	67.95	72.43	63.30
QPLR%	37.36	46.43	62.86	64.78	55.18
V_{min} @ bus	0.93 @ 18	0.9479 @ 32	0.9617 @ 32	0.9650 @ 14	0.9864 @ 25
V_{max} @ bus	1 @ 1	1@1	1 @ 1	1.017 @ 25	1 .017 @ 7

Figures are drawn for the maximum system loadability, voltage profile, system loss, and voltage stability indices for all the cases under study as Figure 4.14, Figure 4.15, Figure 4.16 and Figure 4.17, respectively. Figure 4.14 shows that the highest maximum system loadability is achieved by implementation of Case 4 compared to other cases under the presence of Q, PQV pair of buses. Figure 4.15 presents voltage profile of all the cases, which shows that voltage magnitudes are lying well within the permissible limits except Case 1 and Case 2. Figure 4.16 shows the real and reactive power loss profile of the system for cases under study. It is observed from Figure 4.16 that minimum loss is achieved with Case 4 compared to all other cases under the presence of Q, PQV pair of buses. Figure 4.17 shows the voltage stability indices of the system buses with the cases under the presence of Q, PQV buses. From Figure 4.17 it is observed that voltage stability indices are improved greatly with Case 5 as compared to other cases.

Consequently, Case 4 awards a considerable enhancement in the performance indices and harvests best maximum loadability at highest voltage profile improvement. The proposed multi-objective algorithm for enhancement of maximum system loadability increases the network loadability with highest reduction in active power loss, with all buses within the specified voltage limits except Case 2.

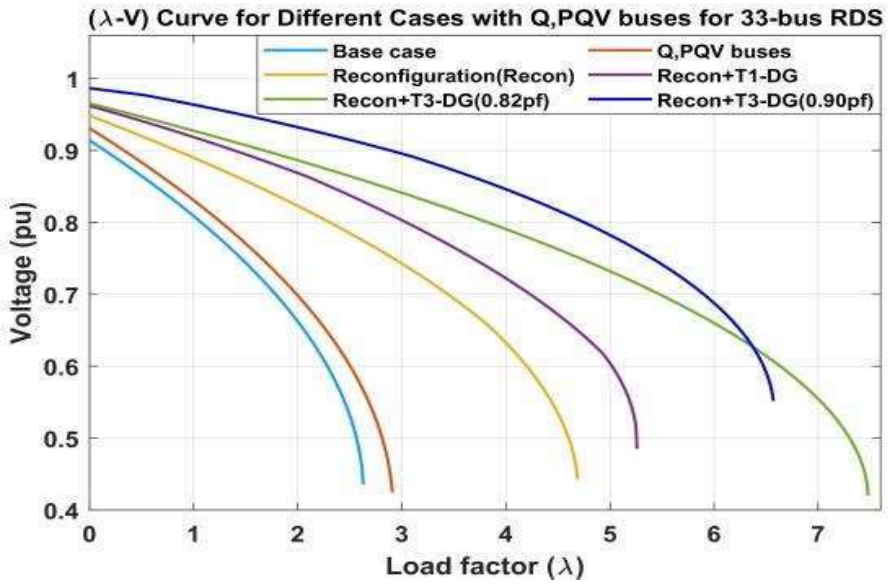

Figure 4.14: Loadability curve for cases with Q, PQV buses for IEEE 33-bus

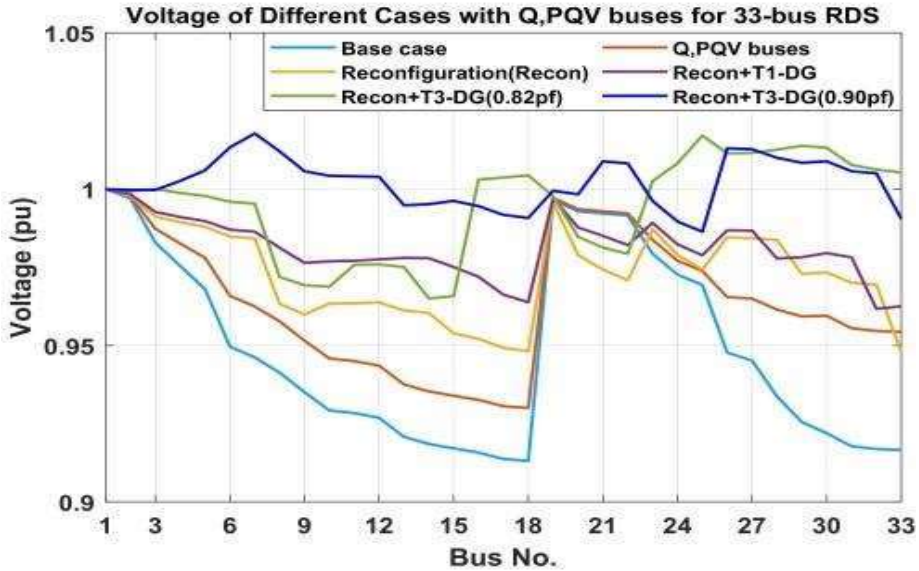

Figure 4.15: Voltage Profile for cases with Q, PQV buses for IEEE 33-bus

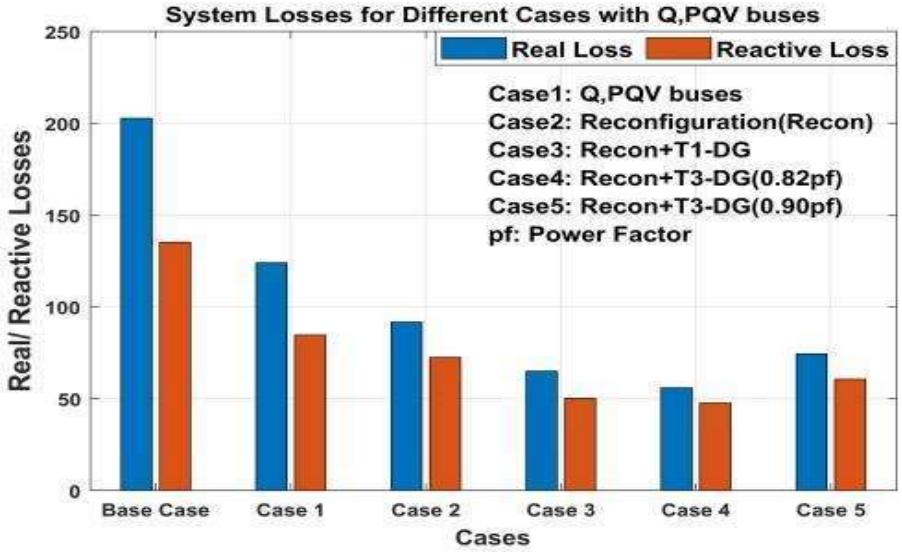

Figure 4.16: Loss Profile of cases with Q, PQV buses for IEEE 33-bus RDS

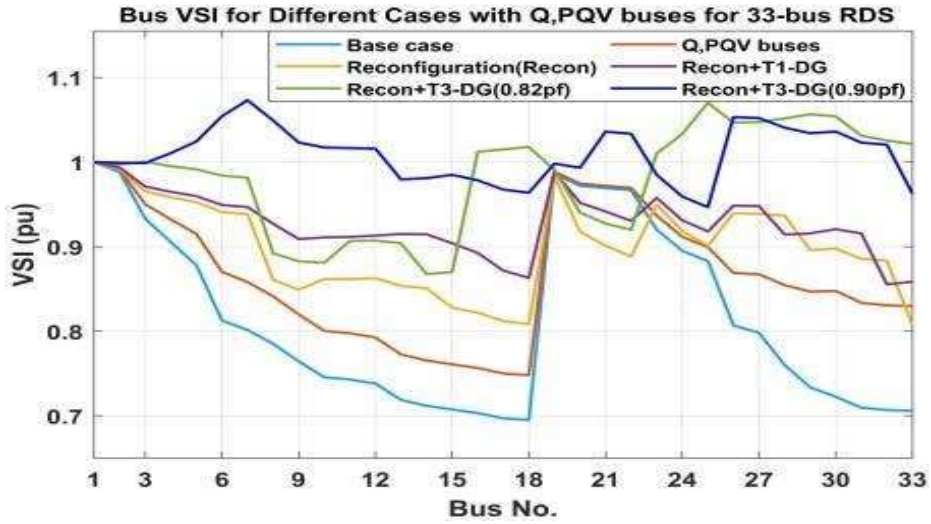

Figure 4.17: VSI of cases with Q, PQV buses for IEEE 33-bus RDS

4.5.2 Test system 2 (69-bus RDS)

4.5.2.1 *Selection of PQV bus*

The PQV bus was selected based on a criterion of being farthest bus having lowest voltage magnitude. Base case voltage magnitudes of all the buses have been shown in Table 4.10. It is observed from Table 4.10 that remote bus 65 has got a voltage magnitude of 0.9092 pu, which is lowest. Therefore, bus 65 was selected as PQV

bus for 69-bus radial distribution system. The pre-defined voltage of PQV bus (bus 65) was set as 0.93 pu for the base case condition. The enhanced voltage was to be obtained through reactive power injection at P bus or real power injection at Q bus.

Table 4.10: Base case voltage magnitude at buses (69-bus RDS)

Bus No.	Voltage magnitude (pu)	Bus No.	Voltage magnitude (pu)	Bus No.	Voltage magnitude (pu)
1	1.0000	24	0.9566	47	0.9998
2	1.0000	25	0.9564	48	0.9985
3	0.9999	26	0.9564	49	0.9947
4	0.9998	27	0.9563	50	0.9942
5	0.9990	28	0.9999	51	0.9785
6	0.9901	29	0.9999	52	0.9785
7	0.9808	30	0.9997	53	0.9747
8	0.9786	31	0.9997	54	0.9714
9	0.9774	32	0.9996	55	0.9669
10	0.9725	33	0.9993	56	0.9626
11	0.9713	34	0.9990	57	0.9401
12	0.9682	35	0.9989	58	0.9290
13	0.9653	36	0.9999	59	0.9248
14	0.9624	37	0.9997	60	0.9197
15	0.9595	38	0.9996	61	0.9123
16	0.9590	39	0.9995	62	0.9121
17	0.9581	40	0.9995	63	0.9117
18	0.9581	41	0.9988	64	0.9098
19	0.9576	42	0.9986	**65**	**0.9092**
20	0.9573	43	0.9985	66	0.9713
21	0.9568	44	0.9985	67	0.9713
22	0.9568	45	0.9984	68	0.9679
23	0.9568	46	0.9984	69	0.9679

4.5.2.2 *Results considering PQV and P buses*

4.5.2.2.(i) Considering multi-objective function proposed in chapter 3

As the primary objective of the work is to enhance the maximum loadability of the RDS and to lower the active power loss, a suitable designation of P bus should be accomplished, accordingly. To designate a P bus, all the buses (except reference bus)

on the feeder connected to PQV bus 65 (minimum voltage bus) are chosen as candidate buses for P bus selection. Each and every bus on this feeder except bus-65 itself are analysed to designate P bus for the maximum voltage stability margin (maximum loadability) and least active power loss. In order to select P bus, a shunt capacitor is connected at a bus and its reactive power output is determined along with VSI_{min}, maximum loadability (λ_{max}) and active power loss (APL) of the system. The procedure is repeated for other buses. The reactive power injection by shunt capacitor, maximum loadability (λ_{max}), voltage stability index at the maximum loadability point VSI_{min} and active power loss (APL) values under shunt capacitor connection at each bus have been shown in Table 4.11.

Table 4.11: P bus Selection for 69-bus RDS

Bus No.	**Shunt Capacitor Injection (MVAr)**	**λ_{max}**	**VSI_{min}**	**APL (kW)**	**Bus No.**	**Shunt Capacitor Injection (MVAr)**	**λ_{max}**	**VSI_{min}**	**APL (kW)**
2	2562.777	3.34	0.7480	19913.37	55	3.7251	3.36	0.7480	232.74
3	1281.359	3.34	0.7480	10042.99	56	3.15998	3.36	0.7480	216.78
4	512.511	3.34	0.7480	4122.55	57	1.9926	3.4	0.7480	179.77
5	87.1763	3.34	0.7480	1419.27	58	1.6691	3.43	0.7480	166.34
6	14.1273	3.34	0.7480	562.17	59	1.56863	3.44	0.7480	161.88
7	7.47045	3.35	0.7480	343.79	60	1.46487	3.46	0.7480	157.41
8	6.6960	3.35	0.7480	317.09	**61**	**1.2812**	**3.48**	**0.7481**	**152.1**
9	6.34416	3.35	0.7480	305.21	62	1.25512	3.48	0.7480	153.03
53	5.36154	3.35	0.7480	278.49	63	1.21891	3.47	0.7480	154.43
54	4.53548	3.36	0.7480	255.51	64	1.06732	3.45	0.7468	160.32

VS_{min} = VSI at maximum loadability point

It is observed from Table 4.11 that connection of shunt capacitor at bus 61 offers the highest maximum loadability, highest voltage stability index, and lowest real power loss

compared to other buses under consideration. Therefore, bus-61 is selected and assigned as the P bus with shunt capacitor injecting 1.2812 MVAr of reactive power. Real and reactive power loss, maximum loadability (λ_{max}) and voltage stability index obtained at the nose point (VS_{min}) have been shown in Table 4.12 in the absence of P, PQV buses and in the presence of P, PQV buses. A significant enhancement of 12.16% has been achieved in maximum system loadability and a significant reduction of 32.39% and 30.91%, respectively, have been obtained in real and reactive power loss, respectively, under selected pair of P bus (bus-61) and PQV bus (bus-65).

Table 4.12: Results before and after selection of P, PQV buses in the IEEE 69-bus RDS

Description	**Q_{sh} @ P bus**	**APL (kW)**	**QPL (kVAr)**	**λ_{max}**	**VSI_{min}**	**V_{min} (pu) & V_{max} (pu)**
Base Case Results (with only PQ buses)	---	224.95	102.14	2.22	0.6833	V_{min} = 0.9092 @ 65 V_{max} = 1.0 @ 1
Base Case Results (with P, PQV buses)	1.2812 MVAr @ 6	152.1	70.57	2.49	0.7581	V_{min} = 0.93 @ 65 V_{max} = 1.0 @ 1

Table 4.12 demonstrates the active power loss, loadability, maximum and minimum voltage of the test system before and after the selection of PQV and P bus in the 69-bus system. It shows that suitably allocating the P bus in the original system not only maintains the desired voltage level of 0.93 pu at the PQV bus but also enhances the performance of overall system in terms of maximum loadability, improved voltage stability index, minimum losses, and improved voltage profile.

Table 4.12 presents results of five cases studied using the multi-objective function proposed in chapter 3 for the system employed with P, PQV buses.

Incorporating P, PQV buses, followed by network reconfiguration by opening the switches associated with set of lines (14, 58, 63, 69, 70) the real power loss drops from

152.1 kW to 74.25 kW, while loadability of the system increases to 4.8 pu. The minimum voltage of the network has improved to 0.9676 pu at bus-64 which is above the set target of 0.93 pu. Further, the application of simultaneous reconfiguration and Type-1 DG (injecting only real power of 2.25792 MW operating at unity power factor) allocation at bus-62 and opening the switches associated with set of lines (17, 22, 54, 69, 71) enhances the loadability of the system to 9.38 pu while keeping the active power loss and reactive power loss to a minimum of 25.13 kW and 13.35 kVAr, respectively. With Case 3, the maximum loadability is improved by 322.52% while the active and reactive power losses are reduced by 88.83% and 86.93%, respectively. In this case, the system minimum voltage magnitude has further enhanced to 0.9798 pu at bus-17.

Further investigations have been carried out with Type-3 DG placed in the system injecting both real and reactive power operating at 0.82 and 0.90 power factors, respectively as Case 4 and Case 5, respectively, as shown in Table 4.13. For Case 4, considering the network reconfiguration and Type-3 DG at 0.82 power factor the optimal solution has been found as DG of 1.8050 MVA placed at bus-62 and opening the switches associated with set of lines (17, 21, 53, 69, 71) increases the system maximum loadability by 583.8% to 14.18, while reducing the real power loss to 43.13 kW and reactive power loss to 27.95 kVAr. The reduction in real and reactive power losses with Case 4 is achieved by 80.83% and 72.64%, respectively. The minimum system voltage has been improved to 0.9802 pu at bus-17. All other indicators for performance have been enhanced. Similarly, for Case 5 DG placement of 2.13318 MVA placed at bus-63 operating at 0.90 power factor, and opening the switches associated with set of lines (15, 21, 57, 69, 71) increases the maximum system loadability by 509.01% to 13.52, while reducing the real and reactive power losses by 80.79% and 78.10% to 40.96 kW and 22.37 kVAr, respectively.

Table 4.13: Results after P and PQV bus consideration for 69-bus RDS

Items	Results with Multi-objective function in chapter 3				
	Case 1	**Case 2**	**Case 3**	**Case 4**	**Case 5**
Open switches	69, 70, 71, 72, 73	14, 58, 63, 69, 70	17, 22, 54, 69, 71	17, 21, 53, 69, 71	15, 21, 57, 69, 71
DG MW/ MVA @ bus	---	---	2.25792 @ 62	1.8050 @ 62	2.13318 @ 63
APL (kW)	**152.1**	**74.25**	**25.13**	**43.13**	**40.96**
QPL (kVAr)	70.57	67.01	13.35	27.95	22.37
λ_{max}	**2.49**	**4.8**	**9.38**	**14.18**	**13.52**
NVVB	8	0	0	0	0
VDI	0.00524	0	0	0	0
VPI	0.06310	0.20950	0.29918	0.32705	0.30001
QLI/QLI$_m$	3.6577	3.7317	3.7953	3.8127	3.7973
APLR%	32.39	66.99	88.83	80.83	81.79
QPLR%	30.90	34.39	86.93	72.64	78.10
V_{min} @ bus	0.93 @ 65	0.9676 @ 64	0.9798 @ 17	0.9802 @ 17	0.9792 @ 16
V_{max} @ bus	1 @ 1	1 @ 1	1.007 @ 62	1.006 @ 62	1.016 @ 63

Figures are drawn for the maximum system loadability, voltage profile, system loss and voltage stability indices for all the cases under study as Figure 4.18, Figure 4.19, Figure 4.20 and Figure 4.21, respectively. Figure 4.18 shows that the highest maximum system loadability is achieved by implementation of Case 4. Figure 4.19 presents voltage profile of all the cases, which shows that voltage magnitudes are lying well within the permissible limits except Case 1. Figure 4.20 shows the real and reactive power losses for cases under study. It can be observed from Figure 4.20 that system loss is lowest for Case 3 compared to all other cases. Figure 4.21 presents voltage stability indices of the system buses for all the cases from which it is observed that minimum VSI has been improved for all the cases and it is highest for Case 4. Looking different aspects, Case 4, here also awards a considerable enhancement in the performance indices and harvests best maximum loadability at highest voltage profile improvement. The proposed multi-objective algorithm for enhancement of maximum system loadability increases the

network loadability with reduction in active power loss and all buses within the specified voltage limits for all the cases studied except Case 1.

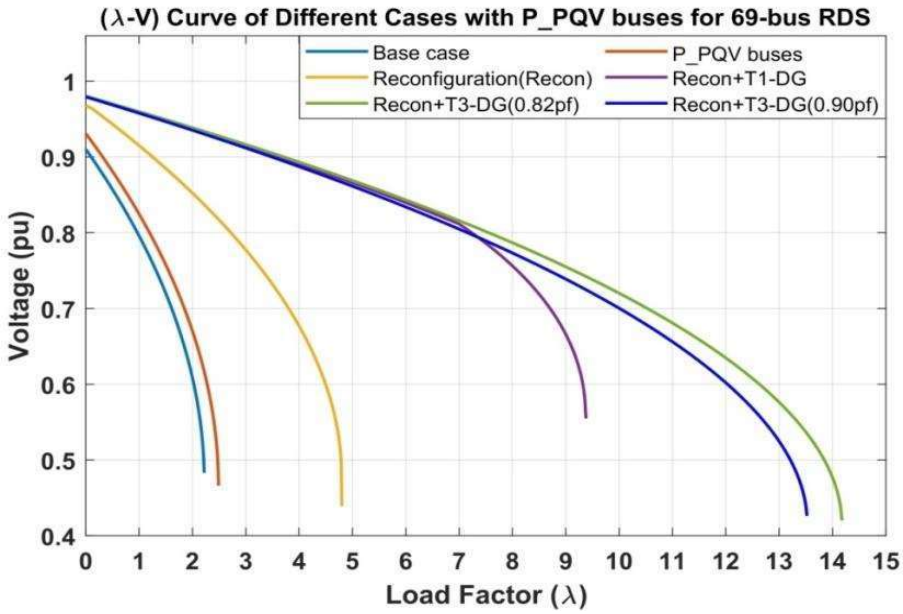

Figure 4.18: Loadability curve for different cases with PQV and P buses for 69-bus RDS

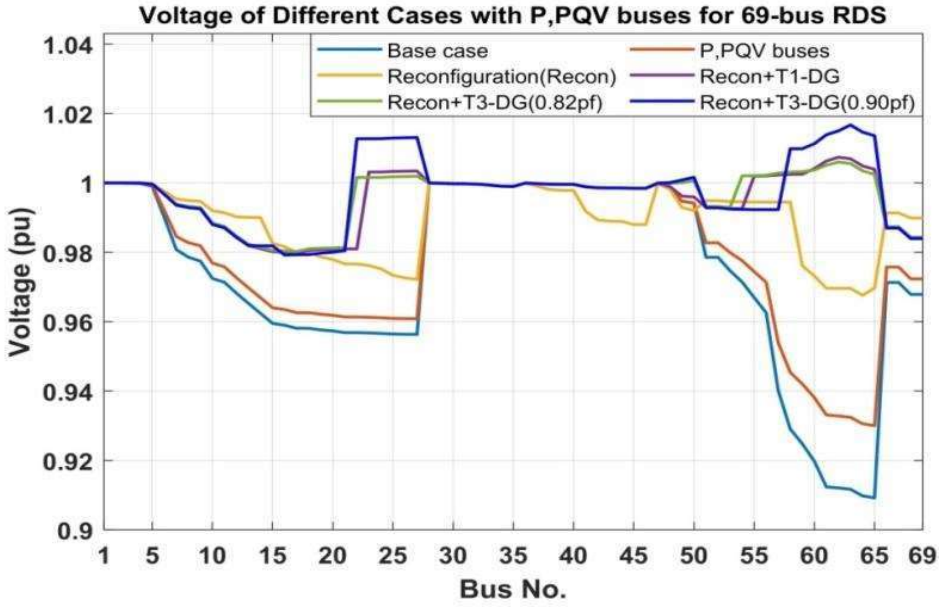

Figure 4.19: Voltage profile for different cases with PQV and P buses for 69-bus RDS

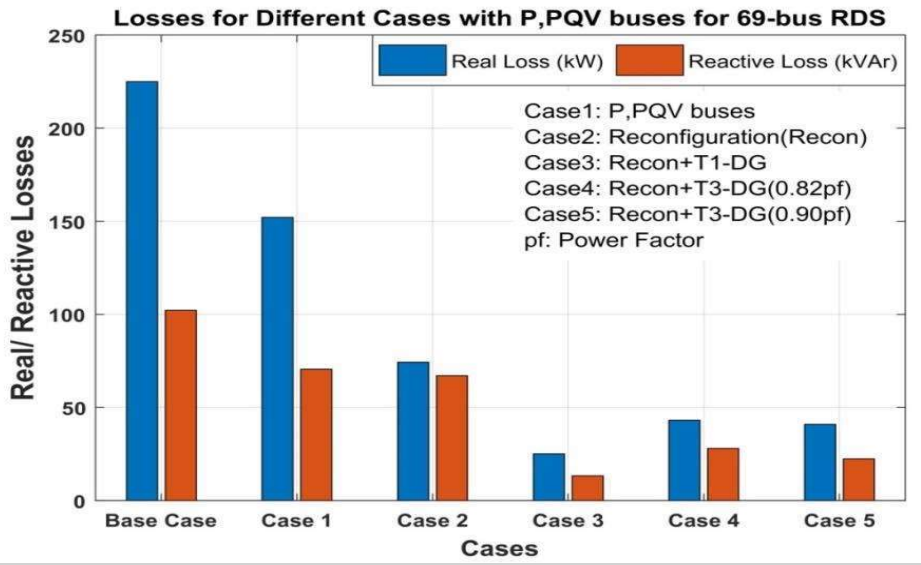

Figure 4.20: System Losses of cases with P, PQV buses for IEEE 69-bus RDS

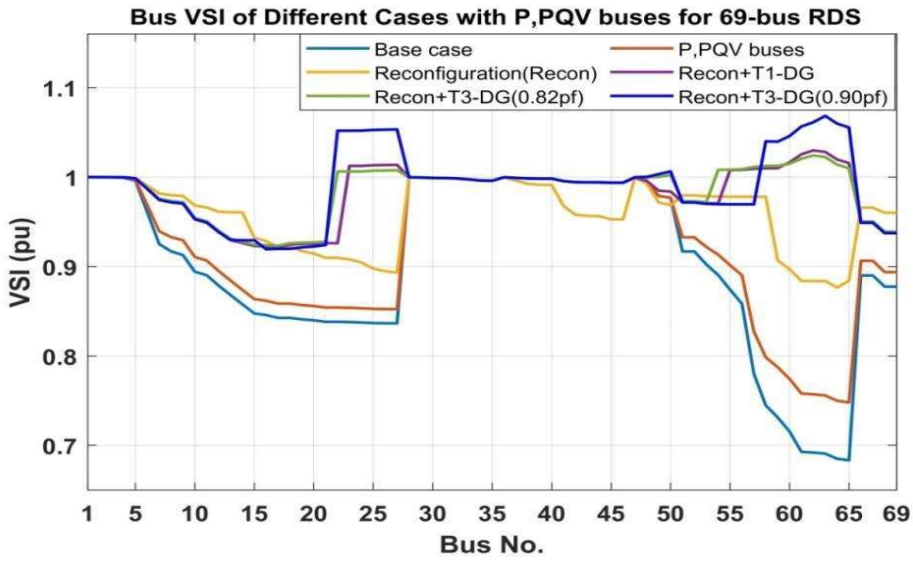

Figure 4.21: VSI for different cases with PQV and P buses for 69-bus RDS

4.5.2.2.(ii) Considering new multi-objective function proposed in this chapter

For selection of a P bus, the optimization procedure is performed with connection of shunt capacitor at each bus considered at a time. The bus with minimum value of fitness function defined by equation (4.15) is selected as P bus. The objective function considers both reduction in real power loss and enhancements in load

quality to be served that ultimately enhance the maximum system loadability. Figure 4.22, shows the real and reactive power loss of the system, QLI and reactive power injected through shunt capacitor connected at the bus under consideration as P bus. In Figure 4.22, results are presented for every possible bus to be assigned as P bus to keep the desired voltage level of 0.93 pu at PQV bus-65. It is observed that consideration of bus-61 as P bus minimizes the multi-objective function with minimum real power loss and enhanced QLI with higher maximum loadability. Therefore, bus-61 is selected and assigned as the P bus with shunt capacitor injecting 1.2812 MVAr of reactive power as shown in Table 4.14. Table 4.14 also shows real and reactive power loss, maximum loadability, minimum voltage stability index and, minimum and maximum voltage of the system in the absence of P, PQV buses as well as in the presence of P, PQV buses. It is observed from Table 4.14 that choosing bus-61 as P bus yields maximum system loadability and real and reactive power loss of the system as 2.49, 152.1 kW and 70.57 kVAr, respectively, and minimum value of VSI as 0.7481. A significant enhancement of 12.16% has been achieved in maximum system loadability and a significant reduction of 32.39% and 30.91%, respectively, have been obtained in real and reactive power loss, respectively, with the incorporation of selected P, PQV buses in the system.

Table 4.14: Results before and after selection of P, PQV buses in the IEEE 69-bus RDS

Description	**Q_{sh} @ P bus**	**APL (kW)**	**QPL (kVAr)**	**λ_{max}**	**VSI_{min}**	**Vmin (pu) & Vmax (pu)**
Base Case Results (with only PQ buses)	-----	224.95	102.14	2.22	0.6833	V_{min} = 0.9092 @ 65 V_{max} = 1.0 @ 1
Base Case Results (with P, PQV buses)	1.2812 MVAr @ 61	152.1	70.57	2.49	0.7481	V_{min} = 0.93 @ 65 V_{max} = 1.0 @ 1

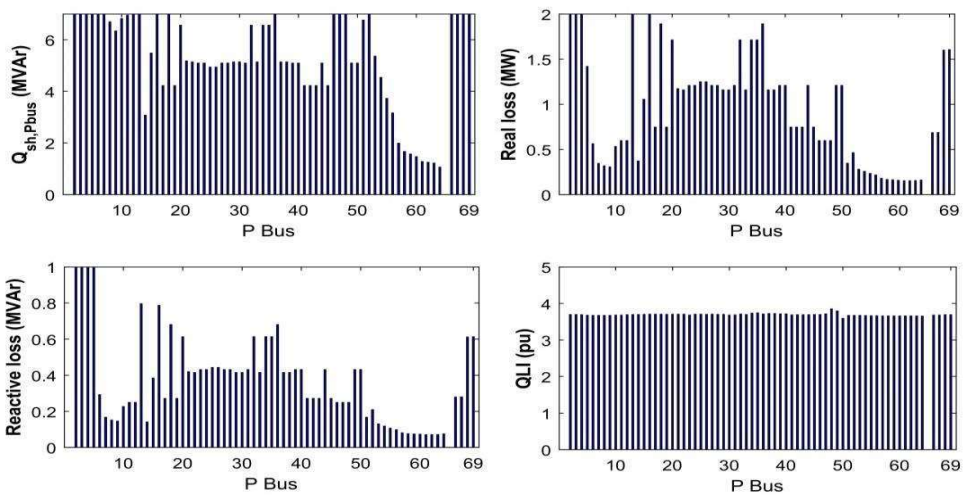

Figure 4.22: P bus selection Criterian for IEEE 69-bus RDS

Table 4.15 presents different performance indices for the five cases considered of the 69-bus system incorporating P, PQV buses by proposed method. Incorporating P, PQV buses, followed by network reconfiguration by opening the switches associated with set of lines (14, 57, 62, 69, 70), the real power loss drops from 152.1 kW to 74.25 kW, while maximum loadability of the system increases to 4.8 pu by 116.22%. The minimum voltage of the network has improved to 0.9676 pu at bus-63 which is above the set target of 0.93 pu. Further, the application of simultaneous reconfiguration and Type-1 DG (injecting only real power) allocation of size 2.25638 MW at bus-62 enhances the loadability of the system to 9.48 pu while keeping the active power loss to a minimum value of 18.72 kW, and reactive power to 12.15 kVAr, thus improves the loadability by 327.03% while real and reactive power losses are reduced by 91.68% and 88.1%, respectively. In this case, the voltage has further enhanced to 0.9885 pu at bus-19.

As depicted in Table 4.15, further investigations have been carried out under Type-3 DG in the system injecting both real and reactive power operating at 0.82 power factor (Case 4), and 0.90 power factor (Case 5), respectively. For Case 4, considering the simultaneous network reconfiguration and Type-3 DG at 0.82 power factor, the optimal

solution has been found as DG of 1.84736 MVA placed at bus-62 and opening the switches associated with set of lines (14, 23, 54, 69, 70) increases the system maximum loadability by 659.46% to 16.86, while reducing the network real and reactive power losses to 37.86 kW and 26.80 kVAr, respectively. In this case, the real and reactive power losses have been reduced by 83.17% and 73.76%, respectively. The minimum system voltage has been improved to 0.9896 pu at bus-22. All other indicators for performance have also been enhanced. Similarly, for Case 5, placing a DG of 1.98855 MVA at bus-63 operating at 0.90 power factor and opening the switches associated with set of lines (13, 18, 22, 54, 69) increases the maximum system loadability by 663.06% to 16.94, while reducing the real and reactive power losses to 31.92 kW and 19.56 kVAr, respectively. The real and reactive power losses have been reduced by 85.81% and 80.85%, respectively, with Case 5. The Case 5 proves to be a highly favourable solution as it enhances the system performances mostly compared to all other cases under study, considering P, PQV pair of buses for 69-bus reconfigurable distribution system.

Table 4.15: Results after P and PQV bus consideration for IEEE 69-bus RDS

Items	**Results with new multi-objective function**				
	Case 1	**Case 2**	**Case 3**	**Case 4**	**Case 5**
Open switches	69, 70, 71, 72, 73	14, 57, 62, 69, 70	12, 18, 21, 58, 69	14, 23, 54, 69, 70	13, 18, 22, 54, 69
DG MW/ MVA @ bus	---	---	2.25638 @ 62	1.84736 @ 62	1.98855 @ 63
APL (kW)	**152.1**	**74.25**	**18.72**	**37.86**	**31.92**
QPL (kVAr)	70.57	67.01	12.15	26.80	19.56
λ_{max}	**2.49**	**4.8**	**9.48**	**16.86**	**16.94**
NVVB	8	0	0	0	0
VDI	0.00524	0	0	0	0
VPI	0.06310	0.20395	0.30821	0.312962	0.32595
QLI/QLI$_m$	3.65769	3.73176	3.80095	3.80547	3.80993
APLR%	32.39	66.99	91.68	83.17	85.81

QPLR%	30.90	34.39	88.1	73.76	80.85
V_{min} @ bus	0.93 @ 65	0.9676 @ 63	0.9885 @ 19	0.9896 @ 22	0.9863 @ 19
V_{max} @ bus	1 @ 1	1 @ 1	1.007 @ 62	1.007 @ 62	1.012 @ 63

Figures are drawn for the maximum system loadability, voltage profile, system loss and voltage stability indices for all the cases under study as Figure 4.23, Figure 4.24, Figure 4.25 and Figure 4.26, respectively. Figure 4.23 shows that the highest maximum system loadability is achieved by implementation of Case 5. Figure 4.24 presents voltage profile of all the cases, which shows that voltage magnitudes are lying well within the permissible limits except Case 1. Figure 4.25 shows the real and reactive power loss profile for different cases under study. From Figure 4.25 it can be observed that system loss is lowest for Case 3 compared to other cases. Figure 4.26 presents voltage stability indices of the system buses for all the cases from which it can be observed that minimum VSI is highest for Case 4 compared to other cases. Looking on different aspects, Case 5 awards a considerable enhancement in the performance indices and harvests best maximum loadability at highest voltage profile improvement. The proposed multi-objective algorithm for enhancement of maximum system loadability increases the network loadability with considerable reduction in active power loss, with all buses within the specified voltage limits except Case 1.

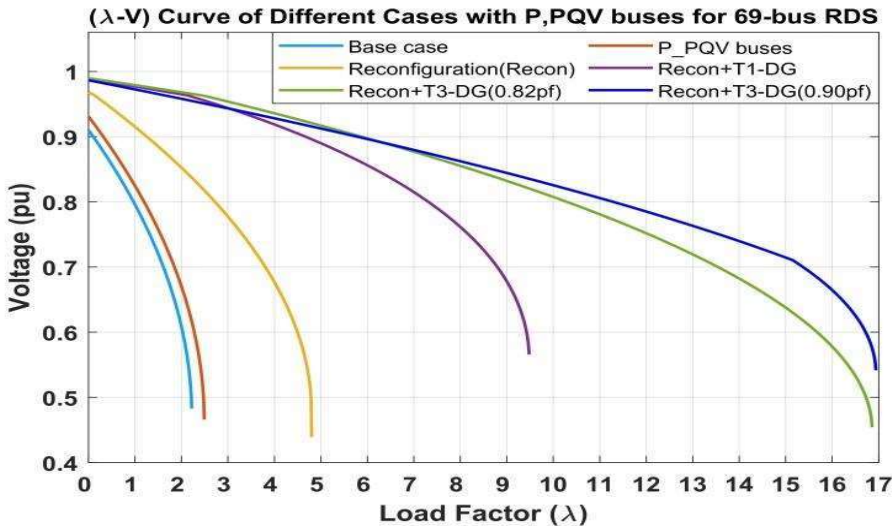

Figure 4.23: Loadability curve of cases with P, PQV buses for IEEE 69-bus RDS

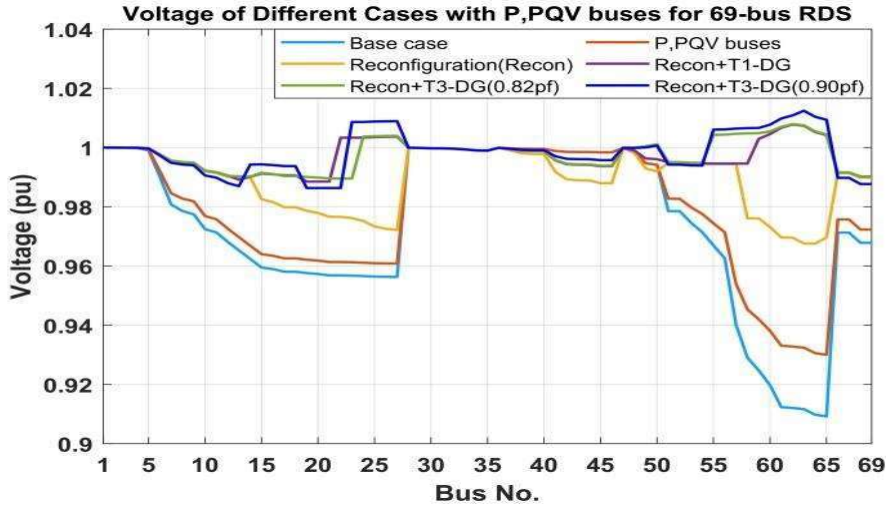

Figure 4.24: Voltage Profile of cases with P, PQV buses for IEEE 69-bus RDS

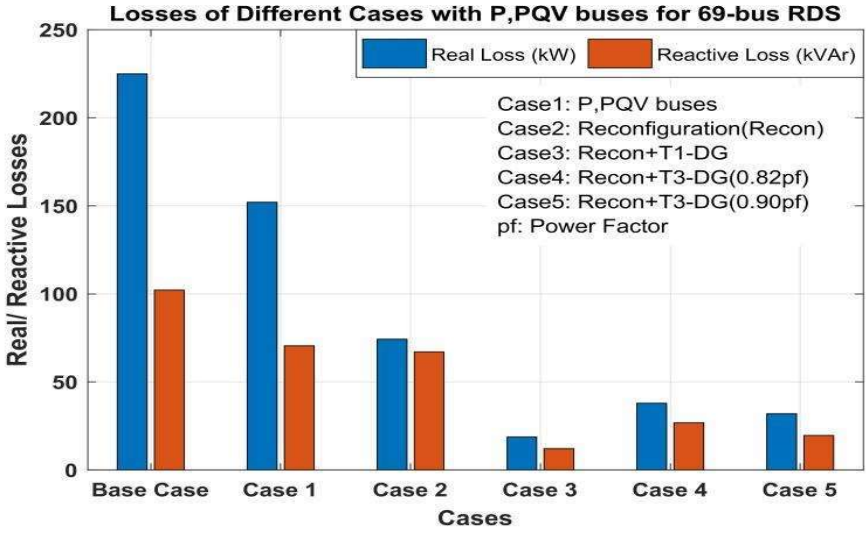

Figure 4.25: System loss of cases with P, PQV buses for IEEE 69-bus RDS

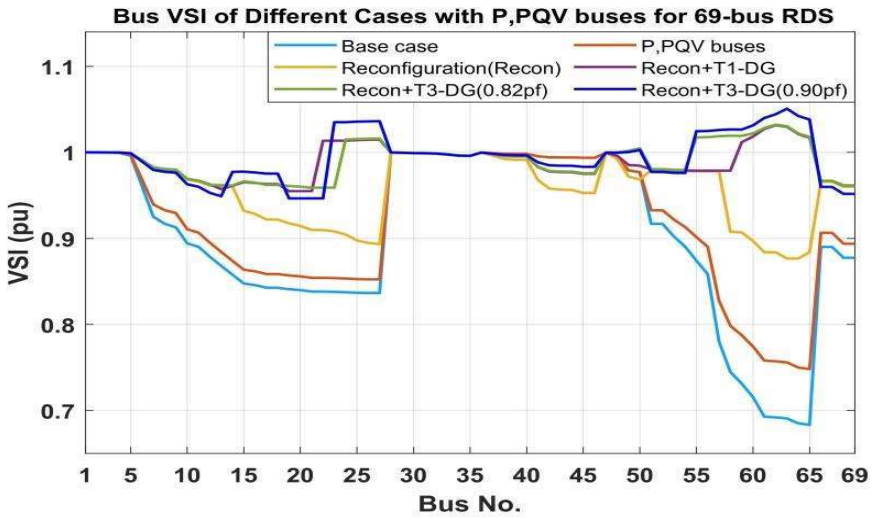

Figure 4.26: VSI of cases with P, PQV buses for IEEE 69-bus RDS

4.5.2.2.(iii) Comparison of results of two multi-objective functions

Table 4.16: Comparison of results for different case with P,PQV buses for IEEE 69-bus RDS

Method/Case		**Open switches**	**DG size @ bus**	**APL(kW)**	**λ_{max}**	**V_{min} @ bus**
Only Reconfiguration (Case 2)	New multi-objective function	**14, 57, 62, 69, 70**	**-----**	**74.25**	**4.8**	**0.9676 @ 63**
	Multi-objective function (chapter 3)	14, 58, 63, 69, 70	---	74.25	4.8	0.9676 @ 64
Reconfiguration and Type-1 DG (Case 3)	New multi-objective function	**12, 18, 21, 58, 69**	**2.25638 @ 62**	**18.72**	**9.48**	**0.9885 @ 19**
	Multi-objective function (chapter 3)	17, 22, 54, 69, 71	2.25792 @ 62	25.13	9.38	0.9798 @ 17
Reconfiguration and Type-3 DG (Case 4)	New multi-objective function	**14, 23, 54, 69, 70**	**1.84736 @ 62**	**37.86**	**16.86**	**0.9896 @ 22**
	Multi-objective function (chapter 3)	17, 21, 53, 69, 71	1.8050 @ 62	43.13	14.18	0.9802 @ 17
Reconfiguration and Type-3 DG (Case 5)	New multi-objective function	**13, 18, 22, 54, 69**	**1.98855 @ 63**	**31.92**	**16.94**	**0.9863 @ 19**
	Multi-objective function (chapter 3)	**15, 21, 57, 69, 71**	**2.13318 @ 63**	**40.96**	**13.52**	**0.9792 @ 16**

Table 4.16 presents the comparison of results obtained by multi-objective function proposed in this chapter with multi-objective function proposed in chapter 3 for enhancing system performances under P, PQV buses. The Table 4.16 shows that system performances have been greatly enhanced in terms of loss reduction and maximum system loadability enhancement with the proposed new multi-objective function in this chapter compared to multi-objective function in chapter 3. The proposed new multi-objective function in this chapter results in a better improvement in terms of real power loss reduction as well as maximum system loadability enhancement compared to multi-objective function proposed in chapter 3 for P, PQV bus allocation under different cases as obtained from Table 4.16.

4.5.2.3 *Results with PQV and Q buses considering new multi-objective function proposed in this chapter*

For selection of a Q bus, the optimization procedure is performed with dispatchable Type-1 DG connected at each bus considered at a time using the fitness function defined by (4.15). The bus with minimum value of fitness function defined by (4.15) is selected as Q bus. The objective fitness function considers both reduction in real power loss and enhancement in load quality to be served that ultimately enhances the maximum system loadability. The bus with minimum value of fitness function defined by equation (4.15) is selected as Q bus. The objective function considers both reduction in real power loss and enhancements in load quality to be served which ultimately enhances the maximum system loadability. Figure 4.27 shows the real and reactive power loss of the system, QLI and real power injected through DG connected at the bus under consideration as Q bus. In Figure 4.27, results are presented for every possible bus to be assigned as Q bus to keep the desired voltage level of 0.93 pu at PQV bus 65. It is observed that consideration of bus-61 as Q bus

minimizes the multi-objective function with minimum real power loss and enhanced QLI with higher maximum loadability. Therefore, bus-61 is selected and assigned as the Q bus with DG injecting 0.5270 MW of real power, as shown in Table 4.17. Table 4.17 also presents real and reactive power loss, maximum loadability, minimum voltage stability index and minimum and maximum system voltage in absence of Q, PQV buses as well as in presence of Q, PQV buses. It has been observed from Table 4.17 that choosing bus-61 as Q bus yields maximum system loadability, and reduced real and reactive power loss of the system as 2.43, 153.19 kW and 71.58 kVAr, respectively, and minimum value of VSI as 0.7481. A significant enhancement of 9.46% has been achieved in maximum system loadability and a significant reduction of 31.90% and 29.92%, respectively, have been obtained in real and reactive power loss, respectively, with the incorporation of selected Q, PQV pair of buses in the system.

Table 4.17: Results before and after selection of Q, PQV buses in the IEEE 69-bus RDS

Description	**P_{DG} @ Q bus**	**APL (kW)**	**QPL (kVAr)**	**λ_{max}**	**VSI_{min}**	**V_{min} (pu) & V_{max} (pu)**
Base Case Results (with only PQ buses)	-----	224.95	102.14	2.22	0.6833	Vmin = 0.9092 @ 65 Vmax = 1.0 @ 1
Base Case Results (with Q, PQV buses)	0.5270 MW @ 61	153.19	71.58	2.43	0.7480	Vmin = 0.93 @ 65 Vmax = 1.0 @ 1

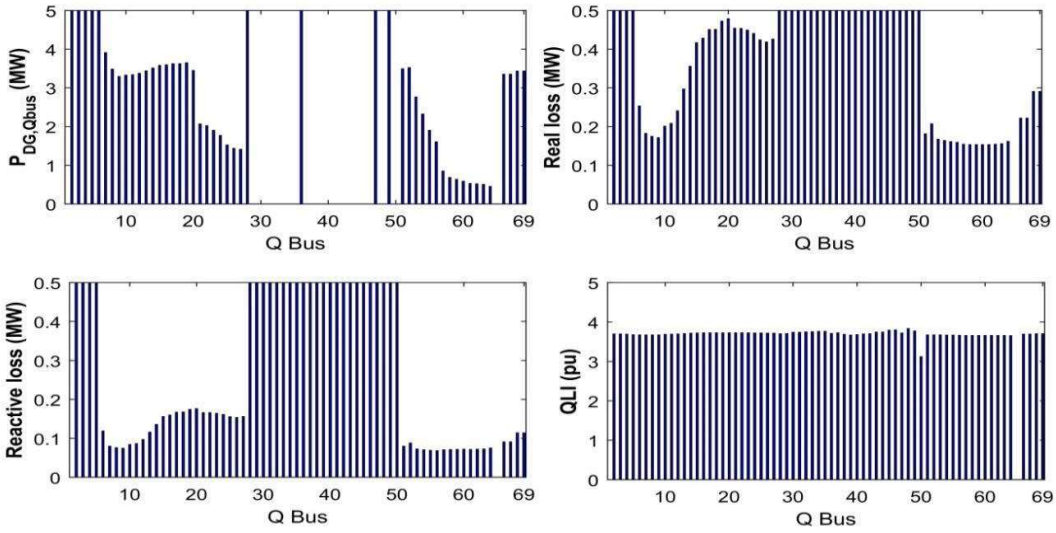

Figure 4.27: Q bus selection criterion for IEEE 69-bus RDS

Table 4.18 presents the performance indices of five cases considered of the 69-bus system incorporating Q, PQV buses by proposed method. Incorporating Q, PQV buses, followed by network reconfiguration by opening the switches associated with set of lines (14, 56, 61, 69, 70) the real power loss drops from 153.19 kW to 69.52 kW, while maximum loadability of the system increases to 4.77 pu. The network reconfiguration in presence of Q, PQV pair of buses enhances the maximum loadability by 114.86%, and real and reactive power losses have been reduced by 69.1% and 35.44%, respectively. The minimum voltage of the network has improved to 0.9615 pu at bus-61 which is above the set target of 0.93 pu. Further, the application of simultaneous reconfiguration and Type-1 DG allocation of size 1.02398 MW at bus-63 enhances the loadability of the system to 7.95 pu while reducing the active and reactive power losses to a value of 51.35 kW and 44.57 kVAr, respectively, thus improving the loadability by 258.11% while the real and reactive power losses are reduced by 77.17% and 56.36%, respectively. In this case, the voltage have further enhanced to 0.9676 pu at bus-64.

Table 4.18: Results after Q, PQV buses consideration for IEEE 69-bus RDS

Items	Results with new multi-objective function				
	Case 1	**Case 2**	**Case 3**	**Case 4**	**Case 5**
Open switches	69, 70, 71, 72, 73	14, 56, 61, 69, 70	14, 58, 63, 69, 70	12, 58, 64, 69, 70	12, 21, 58, 69, 70
DG MW/ MVA @ bus	---	---	1.02398 @ 63	1.62011 @ 62	1.89411 @ 62
APL (kW)	**153.19**	**69.52**	**51.35**	**17.99**	**21.90**
QPL (kVAr)	71.58	65.94	44.57	15.67	17.36
λ_{max}	**2.43**	**4.77**	**7.95**	**16.48**	**15.86**
NVVB	8	0	0	0	0
VDI	0.00522	0	0	0	0
VPI	0.06094	0.18593	0.22639	0.26756	0.28652
QLI/QLI$_m$	3.6567	3.7143	3.7459	3.7797	3.7855
APLR%	31.90223	69.10	77.17215	92.00231	90.26
QPLR%	29.92049	35.44	56.35803	84.66	82.99
V_{min} @ bus	0.93 @ 65	0.9615 @ 61	0.9676 @ 64	0.9831 @ 65	0.9893 @ 21
V_{max} @ bus	1 @ 1	1 @ 1	1 @ 1	1 @ 1	1 @ 62

As depicted in Table 4.18, further investigations have been carried out for Type-3 DG injecting both real and reactive power at 0.82 power factor (Case 4) and 0.90 power factor (Case 5), respectively, while reconfiguring the network simultaneously. For Case 4, considering the network reconfiguration and Type-3 DG at 0.82 power factor, the optimal solution has been reported as DG of 1.62011 MVA placed at bus-62 and opening the switches associated with set of lines (12, 58, 64, 69, 70), and it increases the maximum system loadability by 642.34% to 16.48, while reducing the network loss to 17.99 kW and 15.67 kVAr, respectively. For Case 4, real and reactive power losses have been mostly reduced by 92.01% and 84.66% respectively. The minimum system voltage has been improved to 0.9831 pu at bus-65. All other indicators for performance have also been enhanced as shown in Table 4.18. Similarly, for Case 5, placing a DG of 1.89411 MVA at bus-62 with 0.90 power factor and opening the switches associated

with set of lines (12, 21, 58, 69, 70) increases the maximum system loadability by 614.41% to 15.86 pu, while reducing the real and reactive power losses to 21.90 kW and 17.36 kVAr, respectively. With Case 5 into consideration the network real and reactive power losses have been reduced by 90.26% and 82.99%, respectively. The minimum system voltage magnitude has enhanced to 0.9893 at bus-21 with Case 5. The Case 4 provides a highly favourable solution as it enhances the system performances mostly as compared to all other cases under study, considering Q, PQV pair of buses for 69-bus reconfigurable distribution system.

Figures are drawn for the maximum system loadability, voltage profile, system loss and voltage stability indices for all the cases under study as Figure 4.28, Figure 4.29, Figure 4.30 and Figure 4.31, respectively. Figure 4.28 shows that the highest maximum system loadability is achieved by implementation of Case 4 compared to other cases under the presence of Q, PQV pair of buses. Figure 4.29 presents voltage profile of all the cases, which shows that voltage magnitudes are lying well within the permissible limits except Case 1. Figure 4.30 shows the real and reactive power loss profile of the system for cases under study. It is observed from Figure 4.30 that minimum loss is achieved with Case 4 compared to all other cases under the presence of Q, PQV pair of buses. Figure 4.31 shows the voltage stability indices of the system buses with the cases under the presence of Q, PQV buses. From Figure 4.31 it is observed that voltage stability indices are improved greatly with Case 5 as compared to other cases. Consequently, Case 4 awards a considerable enhancement in the performance indices and harvests best maximum loadability at considerable voltage profile improvement. The proposed multi-objective algorithm for enhancement of maximum system loadability increases the network loadability with highest reduction in active power loss, with all buses within the specified voltage limits except Case 1.

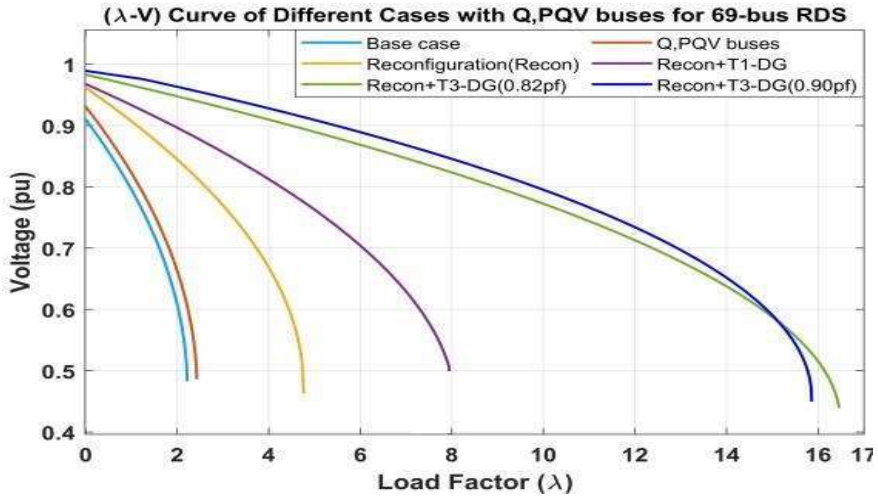

Figure 4.28: Loadability curve of cases with Q, PQV buses for IEEE 69-bus RDS

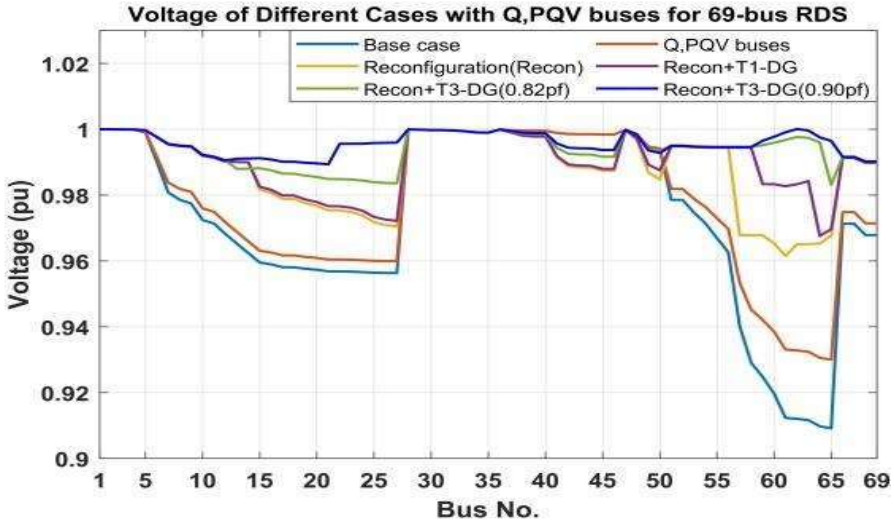

Figure 4.29: Voltage Profile of cases with Q, PQV buses for IEEE 69-bus

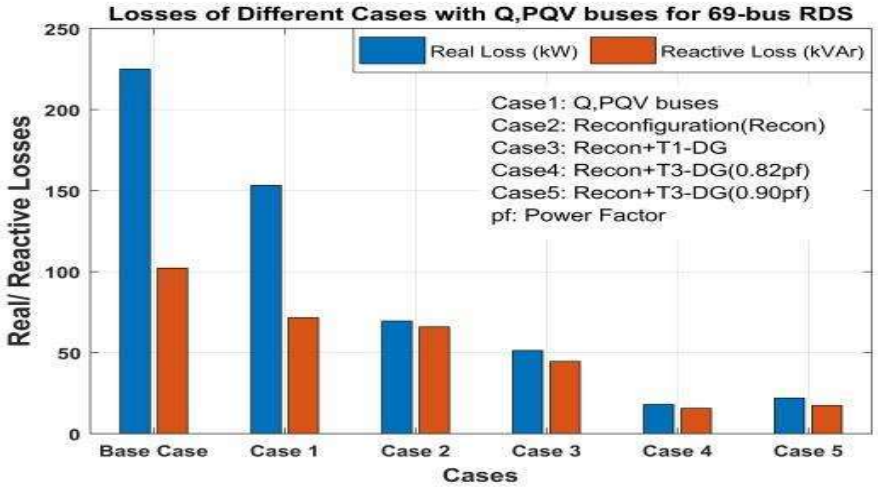

Figure 4.30: Loss Profile of cases with Q, PQV buses 69-bus RDS

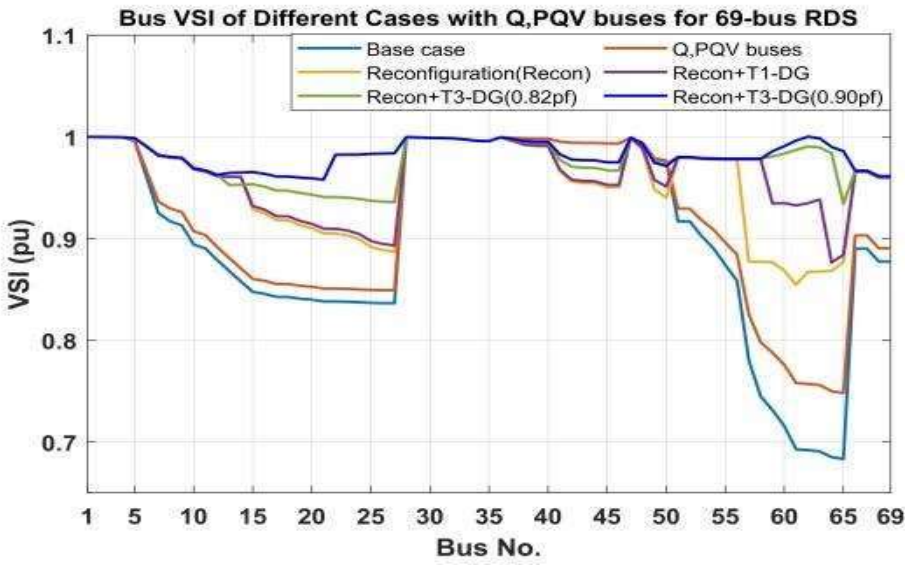

Figure 4.31: VSI of cases with Q, PQV buses for IEEE 69-bus RDS

4.6 SUMMARY

This work has presented a novel approach to reduce the system power loss as well as improve voltage stability in terms of maximum loadability of distribution system with the application P or Q bus controlling the voltage of PQV bus remotely by regulating the reactive power or real power at the bus concerned. A new multi-objective function has been proposed for optimization. The optimal presence of P or Q bus not only enhances the network losses but also results in increased maximum loadability while maintaining the desired bus voltage of novel PQV bus. A P bus that injects reactive power has been found more effective compared to a Q bus that injects real power in terms of overall performance of radial distribution system. Further, network reconfiguration and DG allocation have been found as an effective way to enhance the system performances in terms of loss reduction, maximum loadability enhancement, and voltage profile improvement. It can be observed that better performance is achieved through network reconfiguration and DG placement with the incorporation of P, PQV pair of buses as well as Q, PQV pair of buses in

the system with the proposed objective function. Placement of Type-1 DG, and Type-3 DG at 0.82 power factor and Type-3 DG at 0.9 power factor have been considered in this work. Allocating a Type-3 DG at optimal power factor of 0.82 proves to be more effective in terms of loss reduction and maximum system loadability enhancement as compared to Type-1 DG and Type-3 DG at 0.9 power factor.